

NACA RM E50K22

E 50K22

0143218

TECH LIBRARY KAFB, NM

NACA

RESEARCH MEMORANDUM

EXPERIMENTAL INVESTIGATION OF TAIL-PIPE-BURNER

DESIGN VARIABLES

By W. A. Fleming, E. William Conrad, and A. W. Young

Lewis Flight Propulsion Laboratory
Cleveland, Ohio

Classification cancelled (or changed to

Unclassified)

By Authority of

Nasa Tech Pub Announcement #122
(OFFICER AUTHORIZED TO CHANGE)

By

3 Dec 51

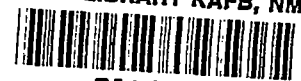
NK

GRADE OF OFFICER MAKING CHANGE)

29 Mar 61

NATIONAL ADVISORY COMMITTEE
FOR AERONAUTICSWASHINGTON
March 5, 1951

519.98/13



NACA RM E50K22

NATIONAL ADVISORY COMMITTEE FOR AERONAUTICS

RESEARCH MEMORANDUMEXPERIMENTAL INVESTIGATION OF TAIL-PIPE-
BURNER DESIGN VARIABLES

By W. A. Fleming, E. William Conrad, and A. W. Young

SUMMARY

The results of several experimental tail-pipe-burner investigations conducted at the NACA Lewis laboratory during the past few years are summarized to indicate the effects of tail-pipe-burner design variables on the performance and operating characteristics. Numerous tail-pipe-burner configurations were investigated, many of which formed orderly series that permitted studying the effect of a single design variable. Most of the configurations were investigated over a wide range of altitudes and flight Mach numbers.

The data presented indicate the effect of changes in the principal design variables on tail-pipe-burner performance and, within the limits of present knowledge, indicate the desirable design features of a tail-pipe burner that will operate with high combustion efficiency and exhaust-gas temperature up to an altitude of approximately 50,000 feet.

INTRODUCTION

The advent of tail-pipe burning for thrust augmentation of turbojet engines has introduced many new problems in turbojet-engine research. One of these problems is to determine the effects of tail-pipe-burner design variables on the burner performance and operating characteristics. Designers of tail-pipe burners have been handicapped by a lack of specific information that would aid in selecting suitable burner dimensions, flame-holder geometry and size, diffuser shapes, exhaust nozzles, fuel systems, and ignition systems. As a result, designers have often had to resort primarily to trial-and-error experiments based on a meager background of combustion research.

The following requirements must be considered in designing a tail-pipe burner for a given application:

1. Maximum thrust
2. Maximum operable range
3. High combustion efficiency
4. Minimum weight
5. Minimum size
6. Low internal-pressure losses
7. Adequate cooling
8. Good control

Each of these requirements conflicts with one or more of the others and the relative importance of each varies with the particular burner application. Maximum thrust, operable range, and combustion efficiency would logically be obtained under optimum conditions for combustion; that is, when the velocity of the gas entering the combustion zone is low, when there are suitable sheltered regions in which the initial phases of combustion can be sustained, and when the combustion chamber is sufficiently long to permit completion of combustion before the gases leave the exhaust nozzle. On the other hand, minimum weight and size require a burner of small diameter, which will increase the gas velocity, or a short burner length, which will reduce the time available for combustion of the mixture within the burner. Low internal-pressure losses require a good diffuser design, low gas velocities, and the smallest possible flame holder. Provision for cooling requires additional weight and may result in some performance loss. Good control requires a dependable ignition source and a satisfactory continuously variable exhaust nozzle, which poses a formidable problem in regard to cooling and ejector performance.

In order to provide information that would assist designers in selecting the proper configuration to satisfy these burner requirements for a particular application, a research program on tail-pipe burning has been in progress at the NACA Lewis laboratory. Experimental investigations have been conducted on several types of engine with numerous tail-pipe-burner configurations. Some of the results are presented in references 1 to 8. Many of the burner configurations formed orderly series that demonstrated the effect of changing a single design variable, and most of the configurations were investigated over a wide range of simulated altitudes and flight speeds.

Data obtained in the altitude wind tunnel with a representative number of these configurations are summarized in this report to show as clearly as possible the effect of several design variables on the performance characteristics of the tail-pipe-burner arrangements investigated,

and to point out the desirable features in the design of a tail-pipe burner. The variables discussed are flame-holder design, fuel distribution, burner-inlet velocity, combustion-chamber length, tail-pipe cooling, tail-pipe diffusers, variable-area exhaust nozzles, and ignition systems. Over-all performance of a tail-pipe burner that included a number of the desirable design features is also shown.

APPARATUS

Installation

All of the investigations reported herein were conducted with axial-flow-type turbojet engines installed on a wing section in the altitude wind tunnel. A typical engine and tail-pipe-burner installation is shown in figure 1. Dry refrigerated air was provided to the engine through a duct from the tunnel make-up air system. This air was throttled from approximately sea-level pressure to the desired pressure at the compressor inlet, while the static pressure in the tunnel was so maintained as to correspond to the desired altitude. The duct was connected to the engine by means of a slip joint with a labyrinth seal that permitted engine thrust measurements to be made with the tunnel scales.

Burner Configurations

A typical tail-pipe burner is shown in figure 2 to illustrate the location of the burner components. The fuel injectors were located in the diffuser section. Sheltered regions for seating the flame were provided by the downstream end of the diffuser inner body and by the flame holders, which were installed from 3 to 6 inches behind the diffuser inner body. The tail-pipe combustion chambers were cylindrical, except for one series of configurations, and were approximately 4 feet in length, except for those cases in which the effect of combustion-chamber length was being investigated. For most recent investigations, variable-area exhaust nozzles of the clamshell type were used; however, most of the configurations discussed herein were investigated with a fixed conical exhaust nozzle with the area selected to give approximately limiting turbine-outlet temperature when operating with an exhaust-gas temperature of 3000° to 3500° R. An internal liner was installed in some of the burner configurations to provide cooling of the outer shell. This liner extended the full length of the burner section and to within about 2 inches of the exhaust-nozzle outlet.

Two types of fuel injector shown in figure 3 were used. The injectors consisted of flattened radial spray tubes which injected the fuel in impinging jets or in solid jets directed normal to the tail-pipe gas flow. Fuel injectors of these types were selected because it was felt that they would provide the desired fuel and air mixtures with a minimum obstruction in the diffuser passage. In addition, such spray tubes can be quickly constructed or modified without machining operations, permitting convenient control of fuel and air distribution, and requiring no internal fuel manifold. With the first type of spray tube (fig. 3(a)), fuel was injected through impinging jets that provided a flat spray at fuel-supply pressures as low as 20 pounds per square inch. With the second type of spray tube (fig. 3(b)), fuel was injected in solid jets normal to the direction of gas flow. The fuel used in the tail-pipe burners was unleaded gasoline, conforming to specification AN-F-48b, grade 80, and the fuel used in the engines conformed to specification AN-F-32.

The large number of flame holders used in the investigations can be grouped into five general types. Four of the flame-holder types, illustrated in figure 4, comprised a two-ring V-gutter type flame holder, a radial-gutter type flame holder, a semitoroidal type flame holder, and a stage-type fuel-cooled flame holder. These types of flame holder were used in conjunction with the flame seat at the downstream end of the inner cone. The fifth flame-holder type comprised only the inner-cone flame seat, which is referred to as the pilot cone.

The two-ring V-gutter flame holders consisted of two annular gutters joined together by four radial gutters. Flame holders of this type were designed to provide good coverage of the combustion-chamber area without allowing flame to seat near the burner shell. The radial-gutter flame holder consisted of a single annular gutter from which a number of radial gutters extended both toward the center of the burner and toward the outer shell. This type of flame holder was designed to block approximately the same area as the two-ring V-gutter flame holders and at the same time to offer a maximum perimeter from which vortices and circulation could emanate. The semitoroidal flame holder consisted of a single ring having a semicircular cross section with the arc upstream and the downstream side closed. This flame holder blocked approximately 0.60 as much area as the two-ring and radial-gutter flame holders and consequently caused less pressure loss.

The stage-type fuel-cooled flame holder was designed to produce burning in three stages, with each downstream ring partly immersed in flame from the preceding ring. This flame holder was cooled by fuel supplied to each of the rings through the mounting tubes. The fuel was then injected into the gas stream through orifices located at the

2058 leading edge of the rings. Preliminary experiments indicated the desirability of locating the largest of the three rings upstream. With the order of the rings reversed, that is, with the large ring downstream, not only was the burning length for the large ring less, but the blocking effect of the small forward rings forced the air flow toward the outer shell and thereby increased the gas velocity in the region of the large ring, where it was already highest.

The pertinent dimensions and details of the configurations discussed herein are given in table I. These configurations are considered representative of the large number of configurations investigated.

PROCEDURE AND INSTRUMENTATION

Each configuration was evaluated over a range of altitudes and flight Mach numbers at rated engine speed. Because a variable-area exhaust-nozzle that would withstand extended periods of tail-pipe burning was not available at the beginning of the program, fixed-area exhaust-nozzles were used to investigate the design variables. A variable-area exhaust-nozzle was used in the later phases of the program to determine the over-all performance of a burner that included a number of the desirable design features. In order to make the data generally applicable, the operating conditions of the tail-pipe burners are expressed in terms of burner-inlet total pressure, total temperature, and velocity. At each simulated flight condition, the burner was operated over a range of tail-pipe fuel-air ratios from approximately lean blow-out to the fuel-air ratio that gave limiting turbine-outlet temperature. Tail-pipe fuel-air ratio is defined as the ratio of tail-pipe fuel flow to unburned air flow entering the tail pipe, assuming complete combustion of the engine fuel (equation (8), appendix).

The tail-pipe burners were instrumented at the location shown in figure 5. A comprehensive total-pressure and temperature survey was made at the turbine outlet with four to six rakes, depending on the particular engine installation. Static pressure was measured at the burner inlet with four wall orifices, and a water-cooled survey rake was installed at the exhaust-nozzle outlet to measure total and static pressures. Air flow was determined from a survey of total pressure, total temperature, and static pressure at the engine inlet. Engine and tail-pipe fuel flows were individually measured with calibrated rotameters. The manner in which tail-pipe burner performance was calculated from these measurements is discussed in the appendix.

RESULTS AND DISCUSSION

Burner-Inlet Conditions

Typical variations of burner-inlet total pressure, total temperature, and velocity with tail-pipe fuel-air ratio during operation with a fixed-area exhaust nozzle are shown in figure 6 for several altitudes and two flight Mach numbers. Burner-inlet total pressures and temperatures are considered equal to the values measured at the turbine outlet.

At a given altitude and flight Mach number, an increase in tail-pipe fuel-air ratio resulted in a rise in burner-inlet total pressure and total temperature accompanied by a slight reduction in burner-inlet velocity. An increase in altitude or reduction of flight Mach number at a given tail-pipe fuel-air ratio lowered the burner-inlet total pressure and raised the burner-inlet velocity. For some other engines, a variation in flight conditions had no appreciable effect on burner-inlet velocity. Because the variation of burner-inlet total temperature with altitude and flight Mach number is primarily dependent on the tail-pipe combustion efficiency, the trends of burner-inlet temperature with altitude and flight Mach number shown in figure 6 are not general for all configurations.

The exhaust-nozzle area for each series of configurations was chosen, as mentioned previously, to give limiting turbine-outlet temperature when operating at exhaust-gas temperatures of 3000° to 3500° R. At low tail-pipe fuel-air ratios, therefore, where the turbine-outlet temperature was 200° to 400° F below the limiting value, the combustion efficiencies obtained may be lower than those obtainable with a variable-area exhaust nozzle that would permit operation at limiting turbine-outlet temperature for all tail-pipe fuel-air ratios. Performance near limiting turbine-outlet temperature was unaffected, however, and comparison of trends of the data obtained with each series of burner configurations having the same exhaust-nozzle area is valid.

In the succeeding figures, the maximum fuel-air ratio represents operation at approximately limiting turbine-outlet temperature with the particular size exhaust-nozzle used, and the minimum fuel-air ratio represents operation near the lean blow-out limit. Except where otherwise noted, the burner operating conditions in the succeeding figures are expressed as the range of burner-inlet pressures and the average burner-inlet velocity between these fuel-air ratio limits.

Flame Holders

2058

Effect of flame-holder arrangement. - In the design of a tail-pipe burner, flame-holder design is one of the primary factors to be considered. Study of this design variable included an evaluation of a large number of flame holders having different geometries and blocked areas. The performance of seven configurations (series A and B, table I) are summarized in figures 7 to 9 to indicate the effect of flame-holder design on burner performance. The four series A flame holders were investigated in a 29-inch-diameter tail-pipe burner having an inlet velocity of approximately 420 feet per second, and the three series B flame holders were investigated in a 32-inch-diameter burner (installed on a different engine) with burner-inlet velocities from 425 to 515 feet per second.

Because of the difference in burner-inlet velocity, comparisons between the data of figures 7 and 8 are not valid; however, comparisons of the data within either figure may be made to indicate the effect of flame-holder type on combustion efficiency. At burner-inlet total pressures of 2500 to 3400 pounds per square foot (fig. 7(a)) the peak combustion efficiencies obtained with the four types of flame holder were within about 0.05 of each other. It is noted that the peak efficiency with the stage-type fuel-cooled flame holder occurred at a tail-pipe fuel-air ratio of approximately 0.029, whereas the peak efficiency of the other flame holders occurred at tail-pipe fuel-air ratios in the region of 0.04. This trend was more apparent in data not included, which showed that the combustion efficiency of the fuel-cooled flame holder rapidly decreased in comparison with those of the other flame holders at fuel-air ratios above approximately 0.035. This decrease in combustion efficiency was probably due to fuel being injected close to the gutters, thereby producing a stoichiometric mixture in that region at relatively low over-all tail-pipe fuel-air ratios, whereas for the other flame holders fuel was more uniformly distributed at a station some distance upstream. The rapid decrease in combustion efficiency above a tail-pipe fuel-air ratio of 0.035 precludes operation of the fuel-cooled type of flame holder at high fuel-air ratios with high exhaust-gas temperature.

When burner-inlet total pressure was reduced, corresponding to operation at higher altitudes, the effect of flame-holder design became more apparent. Reducing the burner-inlet total pressure to values between 400 and 600 pounds per square foot (fig. 7(b)) slightly lowered combustion efficiency of the two-ring V-gutter type flame holder, markedly lowered combustion efficiency of the semitoroidal flame holder, and resulted in a very weak flame with attendant low combustion efficiency for the pilot-cone flame holder. Combustion was not obtainable with the fuel-cooled flame holder at these pressures.

CONFIDENTIAL

The combustion efficiencies obtained with the configurations operated at burner-inlet velocities of 475 to 515 feet per second (fig. 8) were similarly reduced as burner-inlet pressure was lowered. At inlet pressures between 1275 and 1400 pounds per square foot, the two-ring V-gutter had the highest combustion efficiency and the pilot-cone flame holder had the lowest.

During operation at burner-inlet pressures between 425 and 525 pounds per square foot, a sudden rise in combustion efficiency sometimes occurred from a low to a considerably higher level, and the two-ring V-gutter and the radial-gutter flame holders could be operated over a range of fuel-air ratios at two levels of combustion efficiency, as shown in figure 8(b). This phenomenon is explainable from observations of the flame through a periscope; these observations indicated that immediately following a start at low burner-inlet pressures with low tail-pipe fuel-air ratios, the flame seated only on the pilot cone with the radial-gutter flame holder installed, and on the pilot cone and inner ring of the flame holder with the two-ring V-gutter type flame holder installed. As the tail-pipe fuel-air ratio was increased, with an attendant rise in burner-inlet temperature and pressure, conditions for combustion were progressively improved until the flame propagated outward to the remaining flame-holder surfaces, resulting in a marked improvement in combustion efficiency. With the flame then seated on the entire flame holder, it was possible to reduce tail-pipe fuel-air ratio to relatively low values at the higher combustion-efficiency level. Such operation at the higher efficiency level and reduced tail-pipe fuel-air ratios probably resulted from the higher burner-inlet temperature and pressure and the beneficial effects of the hot metal surfaces of the flame holder and the burner liner. The pilot-cone flame holder was inoperative at burner-inlet pressures between 425 and 525 pounds per square foot.

Performance of the several flame-holder types is compared in figure 9, in which the variation of peak combustion efficiency with burner-inlet total pressure is shown for each flame holder. As indicated by these data, higher combustion efficiencies were obtained with the two-ring V-gutter type flame holders having a blocked area of about 30 percent than with any other type investigated, particularly at the lower pressures. At low altitudes corresponding to burner-inlet pressures above approximately 2000 pounds per square foot, combustion efficiency was not greatly affected in most cases by flame-holder type. As might be expected, the pilot-cone flame holder having the same fuel system used with each of the other flame holders (except the fuel-cooled flame holder) had the lowest combustion efficiency at all altitudes. Nevertheless, flame holders having low blocked area, such as the pilot-cone or semitoroidal flame holders, may be most suitable for installations requiring tail-pipe burning only at take-off or at low altitudes.

With such an installation, the slight sacrifice in combustion efficiency at these operating conditions may be outweighed by the reduced tail-pipe pressure losses during the remainder of the flight with the burner inoperative. It should be noted that as the burner-inlet total pressure was raised above approximately 2200 pounds per square foot, a slight reduction in combustion efficiency occurred with some of the flame holders. The reason for this reduction is not fully understood, although it is attributed to a change in the fuel-air ratio distribution with altitude as a result of the variation in fuel injection pressure and turbine-outlet flow distribution.

Effect of gutter width and gutter angle. - With the two-ring V-gutter type flame holders, which were shown to have higher combustion efficiencies than the other flame holders investigated, it has been found that gutter size and gutter angle affect the performance and operating limits. In several investigations at the Lewis laboratory, it has been observed that V gutters measuring $1\frac{1}{2}$ to 2 inches across the open end had significantly higher combustion efficiencies and higher altitude operating limits than smaller gutters. An isolated investigation with a 3-inch gutter indicated no further improvement in performance.

The effect of gutter angle on combustion efficiency, shown in figure 10, was investigated by operating a tail-pipe burner with three different two-ring annular V-gutter flame holders which were identical except for the included angle of the gutters. Annular V gutters having included angles of 20° , 35° , and 50° were used for the three flame holders, with the width across the open end of the gutters maintained at $1\frac{3}{4}$ inches; consequently each blocked approximately 30 percent of the combustion-chamber cross-sectional area. At burner-inlet total pressures of 1275 to 1475 pounds per square foot (fig. 10(a)), variation in gutter angle had only a slight effect on combustion efficiency, but at inlet pressures of 425 to 525 pounds per square foot (fig. 10(b)) the combustion efficiency with a 50° gutter angle was considerably below that with the other two gutter angles. For most conditions, the highest efficiencies were obtained with a 35° gutter angle. These data are summarized in figure 11, in which variation in peak combustion efficiency with gutter angle is shown. The gutter angle giving the highest combustion efficiencies decreased from approximately 35° to 25° as the average burner-inlet pressure was reduced from 1400 to 500 pounds per square foot. The decrease in combustion efficiency that accompanied a reduction in burner-inlet pressure became more pronounced as the gutter angle was increased.

The data thus far presented have indicated that at low burner-inlet pressures the best performance characteristics can be obtained with a two-ring V-gutter type flame holder having a gutter angle of 25° to 35° , a blocked area of 30 percent of the combustion-chamber area, and measuring $1\frac{1}{2}$ to 2 inches across the open end of the gutters. This general flame-holder arrangement was selected for the investigation of the other tail-pipe burner variables discussed in this report.

Fuel Distribution

After a flame holder has been selected, it is necessary to establish the fuel distribution that will give maximum combustion efficiency. Because maximum combustion efficiencies at high fuel-air ratios can be expected with a perfectly homogeneous mixture, the attainment of maximum exhaust-gas temperature, which requires high efficiency at approximately stoichiometric fuel-air ratio, would require that fuel be so injected that the air and fuel mixture is uniform across the burner. Attainment of such a mixture requires that the fuel distribution across the burner be tailored to each engine, because the velocity profile near the turbine outlet, and consequently at the burner inlet, differs from one engine make or model to another. Some typical velocity distributions, measured near the turbine outlet of three different engines, are shown in figure 12. In general, the velocities were highest near the outer wall of the tail-pipe diffuser and decreased near the inner wall, requiring a corresponding radial variation in fuel distribution to obtain a uniform fuel and air mixture.

Another factor taken into account in selecting the fuel distributions used in this investigation was the provision of a layer of fuel-free gas at the burner inlet for the purpose of cooling. Part of this layer passed between the liner and the burner shell and part along the inner wall of the cooling liner. Further refinements in tail-pipe cooling techniques may obviate the need for such a layer of fuel-free gas along the inner wall of the liner.

Effect of radial fuel distribution. - The effect of radial variations in fuel distribution on tail-pipe performance is summarized by the data obtained with two series of injector configurations that were progressively altered to give more nearly homogeneous fuel-air ratio distributions. Location of the fuel-injection orifices for these configurations is shown in figures 13 and 14, which are drawn to scale, and the performance with these locations are compared in figures 15 and 16. For one series of configurations (fig. 13), fuel was injected into the annular diffuser through 12 streamlined spray tubes, similar to those

illustrated in figure 3, located $10\frac{3}{4}$ inches upstream of the flame holder. Injection of fuel fairly close to the inner cone with these two configurations resulted in a rich fuel-air mixture at the center of the burner. This rich zone was found desirable for providing a stable flame on the pilot cone. For the other series of configurations, a conical diffuser was inserted between the outlet of the annular diffuser and the burner inlet. The fuel injectors (fig. 14) were installed in the conical diffuser $20\frac{5}{8}$ to $23\frac{5}{8}$ inches upstream of the flame holder. This slight difference in mixing length among the three configurations of series E was considered to have no significant effect on the performance. With this series of configurations, fuel was injected through 20 conical spray nozzles for configuration E1 and through 20 streamlined spray tubes for configurations E2 and E3. With the D series of configurations (fig. 13), the gas velocities were highest near the outer wall of the diffuser, whereas, with the E series (fig. 14), the highest velocities were near the center of the flow passage due to flow separation at the juncture of the annular and conical diffuser sections.

Progressively altering the injectors for both series of configurations so as to obtain a more homogeneous fuel and air distribution raised the peak combustion efficiency at each burner-inlet pressure and shifted the region of peak combustion efficiency to a higher fuel-air ratio (figs. 15 and 16). Both factors contributed to the attainment of higher exhaust-gas temperatures. The improved performance at high fuel-air ratios was obtained, however, with a sacrifice in combustion efficiency at the low fuel-air ratios. These trends indicate the necessity of a dual fuel-injection system if high combustion efficiencies are required over a wide range of fuel-air ratios. Such a dual injection system should provide locally rich mixtures in the region of the flame-holder gutters for low fuel-air ratio operation and a uniform mixture for high fuel-air ratio operation.

Effect of direction of fuel injection. - In order to determine whether the direction in which the fuel was injected into the gas stream by the spray tubes had any effect on combustion efficiency, fuel was injected in an upstream direction, a downstream direction, and from either side of the spray tubes normal to the direction of flow. The results obtained (fig. 17) indicated no apparent effect of the direction of fuel injection on combustion efficiency. Absence of any effect is indicative of poor penetration of the fuel jets injected upstream or normal to the gas flow because of the high stream velocity. A relatively large number of spray tubes may therefore be required to obtain circumferential uniformity of distribution.

Effect of mixing length. - It was felt that increasing the mixing length between the fuel injectors and the flame holder, thereby allowing more time for vaporization of the fuel, might improve combustion efficiency. The effect of so increasing the fuel mixing length from $17\frac{1}{2}$ to $25\frac{1}{2}$ inches is shown in figure 18. At burner-inlet total pressures of 1200 to 1425 pounds per square foot, the peak combustion efficiency was raised only about 5 percent by this increase in mixing length; however, at burner-inlet total pressures of 450 to 525 pounds per square foot, the peak combustion efficiency was raised 35 percent, indicating the desirability of long mixing lengths, particularly at low burner-inlet pressures.

Burner-Inlet Velocity

The detrimental effect that high velocities have on combustion efficiency is recognized. Uncertainty has existed, however, concerning what velocities might be considered high for a tail-pipe burner and how serious high inlet velocities are. In order to investigate the effect of burner-inlet velocity, three cylindrical tail-pipe combustion chambers 4 feet long and 29, 32, and 34 inches in diameter, respectively, were successively installed on an engine. Each combustion chamber included a two-ring V-gutter flame holder that blocked 27 to 30 percent of the combustion area and had a gutter width of approximately $1\frac{3}{4}$ inches. All configurations were operated with the same exhaust-nozzle area. In addition, the 29-inch-diameter burner configuration was operated on another engine of different design. Data for three of these configurations with inlet velocities from 420 to 555 feet per second are shown in figure 19.

Within the accuracy of the data, no significant change in combustion efficiency was caused by increasing burner-inlet velocity from 420 to 510 feet per second, except at low tail-pipe fuel-air ratios. At low inlet pressures, however, the combustion efficiency was considerably reduced when burner-inlet velocity was further increased to 560 feet per second. Although the performance data are not available, operation with the fourth configuration at burner-inlet velocities slightly above 600 feet per second was possible at inlet pressures as low as approximately 900 pounds per square foot. Combustion appeared to be unstable at this condition and no operation was possible with this inlet velocity at a burner-inlet pressure of 600 pounds per square foot.

The effect of inlet velocity on tail-pipe burner performance is summarized in figure 20, in which the variation of peak combustion

2058

efficiency and total-pressure-loss ratio with burner-inlet velocity are shown for several inlet pressures. These data show that at low burner-inlet pressures, maximum combustion efficiencies were obtained when the burner-inlet velocity did not exceed 450 to 500 feet per second. At a given burner-inlet velocity, the difference in momentum pressure loss between high and low burner-inlet total pressures was apparently within the accuracy of the data, permitting over-all total-pressure-loss ratio to be represented by a single curve. In addition to the reduction in combustion efficiency with increased burner-inlet velocity, there was an appreciable rise in total-pressure-loss ratio. This increase in total-pressure-loss ratio with increased burner-inlet velocity would be reflected in a lower augmented thrust for a given exhaust-gas temperature. Also, with the burner inoperative, the attendant rise in friction pressure loss would reduce the available thrust. It is therefore desirable from considerations of both combustion efficiency at high altitude and pressure loss to maintain burner-inlet velocity as low as possible.

At high burner-inlet pressures, corresponding to operation at sea level or at low altitudes and high flight speeds, low-frequency flashback into the diffuser or high-frequency screaming combustion sometimes occurred. Operation with screaming combustion has resulted in very severe pressure pulsations that caused damage to the burner. In some instances the flame seated in flow-separation regions on the diffuser inner cone or on the lee side of the struts, thereby immersing the flame holder in flame and causing it to burn out. These problems may be aggravated in burners designed to operate at low inlet velocities, inasmuch as low velocities near the diffuser exit are conducive to flashback. Methods of eliminating flashback or screaming combustion are not yet available; however, improved diffuser design may relieve these conditions. A dual fuel-injection system may also be required to obtain the advantage of upstream injection for high-altitude operation and to reduce the tendency for flashback by injection near the flame holder at low altitudes. Burning on the lee side of the struts has been eliminated by shortening the chord of the struts and so relocating the fuel injectors that fuel was injected downstream of the strut trailing edges.

Combustion-Chamber Length

The effect of combustion-chamber length on tail-pipe combustion efficiency, shown in figure 21, was investigated by using nominal lengths of 2, 4, and 6 feet in otherwise identical burner configurations. These burners were 32 inches in diameter, included a two-ring V-gutter flame holder, and were operated at burner-inlet velocities of 470 to 525 feet per second. At inlet pressures of 1300 to 1450 pounds

per square foot, only slight reductions in combustion efficiency resulted from decreasing the length from 6 to 4 feet, whereas at inlet pressures of 425 to 575 pounds per square foot, this reduction in burner length lowered peak combustion efficiency 33 percentage points. A further reduction in length to 2 feet decreased the peak combustion efficiency approximately 11 percentage points at inlet pressures of 1300 to 1450 pounds per square foot, and at inlet pressures of 425 to 575 pounds per square foot the peak combustion efficiency was only 11 percent.

The effect of combustion-chamber length on peak combustion efficiency and total-pressure-loss ratio is shown in figure 22. At burner-inlet total pressures from 1350 to 2150 pounds per square foot, an increase in burner length from 2 to 4 feet resulted in an increase in peak combustion efficiency of approximately 11 percentage points. A further increase in burner length from 4 to 6 feet produced only slight additional improvements in combustion efficiency. At burner-inlet total pressures from 425 to 525 pounds per square foot, however, where the combustion efficiency was only 11 percent with a 2-foot burner length, increases in nominal burner length from 2 to 4 feet and from 4 to 6 feet raised the combustion efficiency to 25 and 58 percent, respectively. As would be expected, total-pressure-loss ratio rose only slightly, approximately 0.006, as combustion-chamber length was increased from 2 to 6 feet. The increase in tail-pipe combustion efficiency that can be obtained by lengthening a combustion chamber will therefore be accompanied by only a negligible loss in augmented and unaugmented thrust.

Tail-Pipe Cooling

In attempts to obtain maximum thrust and consequently maximum exhaust-gas temperature with tail-pipe burning, cooling of the tail-pipe shell and the exhaust nozzle becomes an important consideration. One method of cooling the tail-pipe shell is to provide a layer of unburned gases at approximately turbine-outlet temperature along the inside of the burner shell. Such a layer of relatively low-temperature gases can be obtained by so distributing the fuel and positioning the flame holder that no burning takes place near the outer wall. This method of cooling is satisfactory when maximum thrust augmentation is not required, such as operation with a center-pilot or single ring flame holder. For operation at maximum obtainable exhaust-gas temperatures, particularly at high altitudes where the fuel is injected well upstream of the flame holder to obtain improved combustion efficiency, control of fuel distribution so as to keep the burning away from the outer shell was difficult. In such cases, the exhaust nozzle and the downstream portion of the burner shell often became overheated.

2058 It was felt that a solution to this problem might be installation of a liner inside the burner shell, as shown in figure 2, with a small radial space between the liner and the shell through which gas at approximately turbine-outlet temperature could be directed. Several such liners were investigated in a tail-pipe burner 4 feet in length incorporating a conical exhaust nozzle. Operation with several liners having radial spacings of $1/2$ to 1 inch between the liner and the burner shell, and extending upstream 2 to 4 feet from the burner outlet indicated that most effective cooling was obtained with a liner extending from the burner inlet to within 2 inches of the exhaust-nozzle outlet and having a radial spacing between the liner and burner shell of approximately $1/2$ inch. A radial spacing of less than $1/2$ inch apparently would be satisfactory from cooling considerations, but structural considerations of the installation dictated this dimension as a practical minimum.

Typical tail-pipe burner-shell and liner temperatures measured at the downstream end of the burner are compared with exhaust-gas temperature in figure 23. The liner extended from the burner inlet to within 2 inches of the exhaust-nozzle outlet with a radial space of $1/2$ inch between the liner and burner shell. Approximately 6 percent of the tail-pipe gas flowed through the radial space. Because a fixed-area exhaust nozzle was used, turbine-outlet temperature increased with exhaust-gas temperature; the results are therefore presented as functions of turbine-outlet temperature. As exhaust-gas temperature was increased to 2900° R, with an attendant rise in turbine-outlet temperature to 1680° R, temperatures of the burner shell and burner liner rose to 1460° and 2120° R, respectively. Although the downstream portion of the inner liner reached temperatures at which the metal strength was greatly reduced, the low stress on the liner precluded rapid failure.

Later investigations at exhaust-gas temperatures up to 3500° R with a cooling liner extending the full length of a tail-pipe burner and fixed portion of a variable-area exhaust nozzle indicated that sufficient cooling was provided to prevent any portion of the outer shell from exceeding a temperature at which it glowed a dull red in darkness. Metal temperatures were not measured during these later investigations; however, it was observed that during such operation the inner liner appeared to be at a yellow heat for a few inches upstream of the exhaust-nozzle outlet. This cooling liner, which is shown in figure 24, was still in satisfactory condition after approximately 40 hours of operation over a range of conditions, including a number of runs at exhaust-gas temperatures between 3000° and 3500° R.

Particular attention must be given the method of supporting such a liner because of differential expansion between the liner and the burner shell, and because over a portion of the liner a higher pressure exists in the cooling passage than in the burning region. After investigating several methods of support, it was found that the use of interlocking, longitudinal stringers along the burner shell and inner liner, as indicated in figure 24, was most satisfactory. This arrangement maintained the liner at the proper distance from the burner shell, yet permitted differential expansion in both the longitudinal and circumferential directions. Because the longitudinal forces on the liner were in the rearward direction, the liner was prevented from shifting longitudinally in the burner shell by the convergence of the exhaust nozzle.

It should be pointed out there there was some heat transfer from the tail-pipe burners to the external air stream, which varied in temperature from 0° to 100° F and flowed over the burner shell at velocities of 25 to 75 feet per second. In addition, there was some radiation to the tunnel wall. Therefore, although the results indicate that an inner liner will provide adequate shell cooling for an exposed installation operating at exhaust-gas temperatures up to 3500° R, it is possible that some external cooling may also be required when the burner is enclosed in a shroud or a nacelle.

Ignition Systems

Igniting the mixture of fuel and air in the tail-pipe burner has proved to be a troublesome problem. Two of the many arrangements of spark plugs and pilot fuel nozzles that have been used are shown in figure 25(a). One ignition system consisted of a very small ram jet located just ahead of the main flame holder. The ram jet had its own inlet diffuser, fuel nozzle, spark plug, and flame holder, and was intended to send a jet of flame back to the main flame holder. A number of different modifications of this arrangement proved completely unreliable. Another arrangement consisted of a spark plug located in a depression at the end of the diffuser inner cone. The spark plug was used to ignite fuel supplied to the pilot region by a separate nozzle in the pilot zone or fuel supplied from the main fuel-spray tubes. This system was effective up to altitudes of 30,000 to 40,000 feet when the spark plug operated but it was difficult to maintain high-voltage insulation inside the tail pipe. When the ignition system did not operate, the stand-by method of igniting the tail-pipe burner fuel was a rapid acceleration of the engine, which resulted in a burst of flame into the tail pipe. This method proved effective but is not good operating procedure.

2058

The most satisfactory scheme for igniting the tail-pipe-burner fuel was an outgrowth of the use of engine accelerations for ignition. With this scheme (fig. 25(b)), as soon as fuel was introduced into the tail-pipe burner, additional fuel was injected into one of the engine combustors for 1/2 to 5 seconds in sufficient quantity to approximately double the fuel-air ratio in that combustor. The momentary rich mixture in the combustor produced a streak of flame in the tail pipe sufficient to ignite the tail-pipe burner fuel; hence the names "hot-streak" or "hot-shot" by which it is known. The location at which the additional fuel is injected does not appear to be important. In some installations the flow through one of the main engine fuel nozzles was momentarily increased, and in other installations the fuel was injected either in a solid jet from an orifice or from a spray nozzle directed through a hole midway down the combustor liner.

Dependable ignition with a number of tail-pipe burner configurations has been obtained with this system at altitudes up to 53,000 feet. As many as 100 to 300 starts have been made on each of several engines using this system for 1/2- to 5-seconds duration. As a result of the thermal lag of the metal surfaces momentarily exposed to the ignitor flame, there has been no sign of damage to the engines on which it was used. Use of the hot-streak ignitor at this laboratory has been confined to engines having can-type combustors; however, satisfactory operation has been obtained elsewhere with engines having annular-type combustors.

With the use of specification AN-F-58 fuel in tail-pipe burners, consistent autoignition has been obtained at turbine-outlet temperatures above 1150° F at an altitude of 25,000 feet and at approximately 1300° F at 50,000 feet. With one burner, the fuel-air ratio required for ignition in this manner was approximately 0.01 at an altitude of 25,000 feet and above 0.03 at an altitude of 50,000 feet. Similar trends were obtained with another burner, although autoignition could be obtained with a slightly lower fuel-air ratio at an altitude of 50,000 feet. Ignition under these conditions is possible because of the relatively low surface-ignition temperature of specification AN-F-58 fuel, 495° F. The fuel previously used almost exclusively in tail-pipe burners at the Lewis laboratory, unleaded gasoline conforming to specification AN-F-48b, has a surface ignition temperature of 570° F. Autoignition was not obtained with AN-F-48b under the minimum conditions at which AN-F-58 ignited. Further experience with autoignition of specification AN-F-58 fuel is necessary to determine whether there are any objectionable characteristics of this ignition scheme such as explosive ignition.

Tail-Pipe Pressure Losses

One factor of importance in selecting a tail-pipe-burner design is the loss in unaugmented thrust. This loss is induced by increased total-pressure losses across the tail-pipe burner and by reductions in effective nozzle-velocity coefficient. The effect of tail-pipe

total-pressure-loss ratio $\frac{P_4 - P_6}{P_4}$ on the ratio of unaugmented net

thrust with no tail-pipe total-pressure losses is shown in figure 26 for several values of effective nozzle-velocity coefficient. These results, which were calculated for an altitude of 30,000 feet and a flight Mach number of 0.8, are based on performance values of current engines operating at normal rated cruise conditions. As shown in figure 26, an increase in total-pressure-loss ratio of 0.05 results in a loss in net thrust of approximately 2.5 percent, and a decrease in velocity coefficient of 0.05 results in a net-thrust loss of approximately 7 percent. Calculations for other flight speeds and altitudes indicate that the results are affected only slightly by changes in flight conditions. As flight Mach number is increased, the effect of velocity coefficient on the thrust ratio increases slightly and the effect of pressure loss remains about the same. As altitude is increased, the effect of these variables on the thrust loss is decreased slightly.

Variable-Area Exhaust Nozzles

One of the items required for efficient thrust modulation of a tail-pipe burner is a continuously variable-area exhaust nozzle. At the present time one of the most promising is the clamshell-type nozzle. The two most important considerations in designing a clamshell nozzle are its efficiency in producing thrust and its durability. High efficiency can be obtained by using a nozzle having a planar outlet and by eliminating leakage between the fixed and movable portions of the nozzle, as discussed in reference 9. Durability can be obtained by providing cooling, by designing the nozzle so that it does not warp or jam, and by providing adequate sealing between the movable and fixed portions of the nozzle.

Several clamshell-type continuously variable-area exhaust nozzles of different designs have been used on tail-pipe burners at this laboratory. Four of the nozzles that have been used are shown in figure 27; nozzles A and B were commercially designed, and nozzles C and D are of NACA design. Nozzles A, B, and C were sealed by thin spring metal strips welded to the fixed portion of the nozzles and

making contact with the movable lips. For nozzle D, the movable lips retracted into the space between the outer shell and cooling liner of the nozzle. Sealing was provided by Inconel braid attached to the outer surface of the movable lips.

When closed or partly closed the outlet of nozzle A was non-planar, which resulted in considerable spreading of the jet parallel to the major axis of the outlet. As a result, considerable thrust loss was encountered with this nozzle as compared with that for a fixed conical nozzle (reference 9). In addition, warpage and inadequate sealing were encountered with this nozzle. After a few minutes of operation with tail-pipe burning, it became impossible to operate the movable lips because of warpage of the nozzle.

For nozzle B, which had a planar outlet in both the open and closed positions, and for which the sealing was improved over that of nozzle A, the effective velocity coefficient was approximately the same as that of a fixed conical nozzle (fig. 28(a)). The effective velocity coefficient is defined as the ratio of thrust measured with the tunnel balance to thrust calculated from rake measurements obtained a short distance upstream of the outlet of the fixed portion of the exhaust nozzle. Although the effective velocity coefficient is slightly higher than the velocity coefficient obtained in the usual manner from pressure measurements at the nozzle inlet, it is felt that the difference is small. Other work indicates that nozzle velocity coefficients are primarily dependent on the manner in which the jet leaves the nozzle exit, therefore, because the differences in nozzle geometry between the fixed- and variable-area nozzles occur downstream of the survey plane, the comparisons are considered valid. When the pressure ratio across the exhaust nozzle was subcritical, below approximately 1.8, the effective velocity coefficient was lowest near the intermediate nozzle position where the outlet was nonplanar. At supercritical pressure ratios, nozzle position had no apparent effect. This nozzle was used for approximately 8 hours of tail-pipe-burning operation without structural failure. For a given pressure ratio across the exhaust nozzle, the thrust was considerably higher with nozzle C than with nozzle A, and was nearly as high as with a conical nozzle (reference 9). Nozzle C also provided reasonably good sealing and was undamaged after 40 minutes of tail-pipe burning.

Nozzle D, which was designed to provide sealing between the fixed and movable portions of the nozzle in a relatively cool region, is most promising with respect to installation in a nacelle or fuselage structure where space is limited in the region of the exhaust nozzle. Effective velocity coefficients for this nozzle and a fixed conical nozzle are compared in figure 28(b). Although scatter of the data

prevent accurate determination of the effective velocity coefficients, the mean value at each pressure ratio appears to approximate that of the fixed conical nozzle. Unlike the other nozzles, sealing between the fixed and movable portions of this nozzle is not essential because any leakage flow passing between the fixed and movable portions is exhausted in a rearward direction. Warpage of the cooling liner near the nozzle outlet occurred after approximately 1 hour of operation with tail-pipe burning; however, considerably longer life should be obtainable by improved design of the cooling-liner support in the exhaust-nozzle section.

Diffusers

Because turbine-outlet gas velocity is for most engines within the range shown in figure 14, the flow must be diffused to approximately half of the turbine-outlet velocity to obtain acceptable burner performance and operation. Design of the tail-pipe diffuser to obtain maximum pressure recovery is therefore important in minimizing losses in both augmented and unaugmented thrusts. The task of efficient diffusion is usually complicated by a radial velocity gradient at the turbine outlet and by the requirement that a minimum length be used for diffusion.

Variation of the over-all friction total-pressure-loss ratio with corrected engine speed measured with the burner inoperative is shown in figure 29 for a tail-pipe burner having two different diffusers installed. The diffuser having the long inner cone was used in configuration J1 for which over-all performance data are presented. A two-ring V-gutter flame holder blocking 30 percent of the cross-sectional area was installed in the burner. Also included in figure 29 are the friction total-pressure-loss ratios for the standard engine tail pipe, the friction total-pressure-loss ratios for one of the diffuser-burner combinations with no flame holder installed, and sketches showing the lines of the diffusers and standard engine tail pipe. The areas of both diffusers increased gradually at the forward end where the velocities were highest, and the inner cones followed the same lines to the station at which the area ratio was 1.3, after which the short cone had a much more rapid area change than the long cone. Area ratio is defined as the ratio of the flow area under consideration to the inlet flow area. The over-all area ratio of the diffusers was 2.10, which gave an average burner-inlet velocity of 465 feet per second at rated engine speed. The diffuser configurations and the standard engine tail pipe were used with an exhaust nozzle that permitted operation at approximately limiting turbine-outlet temperature at rated engine speed with no tail-pipe burning.

Comparison of the data for the two configurations with the flame holders installed indicates that shortening the inner cone and enlarging the pilot zone at the end of the inner cone raised the over-all total-pressure-loss ratio at 97.5 percent of rated speed from 0.046 to 0.053, which corresponds to a net-thrust reduction of less than 0.5 percent. With the flame holder removed from the burner having the short cone diffuser, the total-pressure-loss ratio at rated speed was lowered to 0.031, which was approximately the same as for the standard engine tail pipe. Although installation of the burner in place of the standard tail pipe had a negligible effect on the tail-pipe pressure losses, installation of the flame holder raised the total-pressure-loss ratio of the diffuser-burner combination by 0.02 with an attendant reduction in net thrust of about 1.0 percent.

Typical Performance Characteristics

The over-all performance of a tail-pipe burner including a number of the desirable design features thus far discussed was obtained from reference 7 and is shown in figures 30 and 31 for altitudes of 25,000 and 45,000 feet and several flight Mach numbers. Details of the burner, which included a V-gutter type flame holder, radial spray tubes, a continuously variable-area exhaust nozzle, and a cooling liner, are given in table I (configuration J1). The maximum tail-pipe fuel-air ratios represent operation near limiting turbine-outlet temperature with the variable-area exhaust nozzle completely opened, except at flight Mach numbers above 0.59 at an altitude of 25,000 feet where overheating of the burner shell occurred, and at flight Mach numbers above 1.08 at an altitude of 45,000 feet where maintaining the test conditions became exceedingly difficult. The minimum tail-pipe fuel-air ratios at each flight condition are well above the lean blow-out limit.

At each altitude and tail-pipe fuel-air ratio, the increases in turbine-outlet pressure that accompanied increases in flight Mach number raised combustion efficiency and thereby increased exhaust-gas temperature. At a given fuel-air ratio, the augmented thrust ratio also increased with flight Mach number. At an altitude of 25,000 feet and fuel-air ratios above 0.045, flight Mach number had no apparent effect on specific fuel consumption; at an altitude of 45,000 feet, however, the specific fuel consumption was reduced as flight Mach number was increased. Peak combustion efficiencies occurred at tail-pipe fuel-air ratios between 0.04 and 0.05 and decreased only slightly at higher fuel-air ratios. The trends of exhaust-gas temperature and augmented thrust ratio therefore indicate that further increases in

augmented thrust would be obtained with a larger exhaust nozzle, which would permit operation at higher fuel-air ratios. Peak combustion efficiency decreased from approximately 0.88 to 0.71 as burner-inlet total pressure was reduced from 2254 to 772 pounds per square foot. A further reduction in inlet pressure to 592 pounds per square foot lowered the peak efficiency to 0.58. The highest exhaust-gas temperatures obtained with this configuration were approximately 3500° R at an altitude of 25,000 feet and 3300° R at an altitude of 45,000 feet, with corresponding combustion efficiencies of approximately 0.78 and 0.71.

Typical Operating Limits

The lean blow-out limit shown in figure 32 for a tail-pipe burner operating at a flight Mach number of 0.19 indicates the typical lean limit encountered with a series of tail-pipe burners incorporating the desirable design features previously discussed. These burners were similar to configuration J1 for which performance data are presented, having slight variations in flame-holder and fuel-injector locations. Adjustment of the variable-area exhaust nozzle permitted the lean blow-out limits to be obtained while operating near limiting turbine temperature. An increase in altitude raised the tail-pipe fuel-air ratio at which lean blow-out occurred; operation was possible, however, at fuel-air ratios as low as 0.004 at an altitude of 15,000 feet and 0.013 at 50,000 feet.

With configurations of this type, rich combustion blow-out was not encountered. Maximum tail-pipe fuel-air ratio was limited in most cases by operation at limiting turbine temperature with the variable-area exhaust nozzle fully opened. For some configurations, where at high altitudes the exhaust-gas temperature reached a maximum near stoichiometric fuel-air ratio and no further rise was obtainable at higher tail-pipe fuel-air ratios, operation was not attempted at mixtures richer than that corresponding to the peak exhaust-gas temperature.

CONCLUDING REMARKS

The data presented herein indicate, within the limits of present knowledge, the selection for each design variable appearing necessary for a tail-pipe burner that will operate with combustion efficiencies from approximately 85 percent at low altitudes to approximately 75 percent at an altitude of 45,000 feet. Such a tail-pipe burner

2058 should include a V-gutter flame holder blocking approximately 30 percent of the cross-sectional area, with the gutters having an included angle of 25° to 35° and measuring $1\frac{1}{2}$ to 2 inches across the open ends. A sheltered region at the end of the diffuser inner cone will provide improved flame stability. It is desirable to have a burner-inlet velocity of no more than 450 feet per second, and a constant burner diameter for a distance of 4 to 6 feet downstream of the flame holder. Introducing the fuel as close to the turbine outlet as possible with a spray pattern that gives a nearly homogeneous mixture of fuel and air is extremely beneficial in raising the combustion efficiency at high fuel-air ratios and low inlet pressures. The design should include a cooling liner inside the burner shell to provide maximum shell cooling. In order to obtain efficient thrust modulation, a workable, continuously variable-area exhaust nozzle is offered by the clamshell design with either external or internal eyelids. Finally, a hot-streak ignitor installed in one of the engine combustors will provide dependable tail-pipe-burner ignition.

For installations requiring tail-pipe burning only at take-off or at low altitudes, the burner design requirements are modified. Flame holders such as the pilot-cone flame holder or a single-ring flame holder, blocking 15 to 20 percent of the burner cross-sectional area, may be most suitable because of the low-pressure-loss characteristics when the burner is inoperative. Also, less emphasis need be placed on burner-inlet velocity, burner length, and fuel distribution.

Lewis Flight Propulsion Laboratory,
National Advisory Committee for Aeronautics,
Cleveland, Ohio

APPENDIX - CALCULATIONS

Symbols

A	cross-sectional area, sq ft
B	balance scale force, lb
C_j	effective velocity coefficient, ratio of scale jet thrust to rake jet thrust
D	external drag of installation, lb
D_r	drag of exhaust-nozzle survey rake, lb
F_j	jet thrust, lb
F_n	net thrust, lb
g	acceleration due to gravity, 32.2 ft/sec ²
H	total enthalpy, Btu/lb
H'_f	enthalpy of fuel components in products of combustion, Btu/lb
h_c	lower heating value of fuel, Btu/lb
P	total pressure, lb/sq ft
p	static pressure, lb/sq ft
R	universal gas constant, 53.4 ft-lb/lb °R
T	total temperature, °R
t	static temperature, °R
V	velocity, ft/sec
W	weight flow, lb/sec
γ	ratio of specific heats for gases
η_b	combustion efficiency

2058

ρ density, slugs/cu ft

Subscripts:

- a air
- e engine
- f fuel
- g gas
- m fuel manifold
- t tail-pipe burner
- x inlet duct at slip joint
- 0 free-stream conditions
- 1 engine inlet
- 4 turbine outlet
- 5 burner inlet
- 6 exhaust-nozzle outlet

Methods of Calculation

Exhaust-gas temperature. - Exhaust-gas total temperature was calculated from the tail-pipe rake pressure measurements and the mass gas flow through the tail-pipe burner using the concept of flow continuity, where

$$W_g = \rho_6 A_6 V_{6g} = P_6 A_6 \sqrt{\frac{2\gamma_6}{\gamma_6 - 1} \frac{g}{R t_6} \left[\left(\frac{P_6}{P_6} \right)^{\frac{\gamma_6 - 1}{\gamma_6}} - 1 \right]} \quad (1)$$

and

$$T_6 = \left(\frac{P_6}{P_6} \right)^{\frac{\gamma_6-1}{\gamma_6}} \frac{2 P_6^2 A_6^2 \gamma_6 g}{W_g^2 R (\gamma_6-1)} \left[\left(\frac{P_6}{P_6} \right)^{\frac{\gamma_6-1}{\gamma_6}} - 1 \right] \quad (2)$$

Combustion efficiency. - Tail-pipe combustion efficiency is defined as the ratio of enthalpy rise through the tail-pipe burner to heat content of the tail-pipe fuel, disregarding dissociation of the exhaust gas.

$$\eta_{b,t} = \frac{W_{g,6} H_6 - W_{g,4} H_4}{W_{f,t} h_{c,t}} \quad (3)$$

Because differences in turbine-outlet instrumentation among the several engines used resulted in varying accuracy of the turbine-outlet temperature measurement, the enthalpy at the turbine outlet was expressed as

$$W_{g,4} H_4 = W_a H_1 + W_{f,e} h_{c,e} + W_{f,e} H_{f,m} \quad (4)$$

assuming complete combustion in the engine combustor. The enthalpy at the exhaust-nozzle outlet can be expressed as

$$W_{g,6} H_6 = W_a H_6 + (W_{f,e} + W_{f,t}) H'_{f,6} - W_{f,t} H_{f,m} \quad (5)$$

The enthalpy of the fuel components in the products of combustion $H'_{f,6}$ was determined from the hydrogen-carbon ratio of the fuels by the method explained in reference 10. Substituting equation (4) and (5) into equation (3), and thereby crediting the tail-pipe burner only for the enthalpy rise due to the tail-pipe fuel gives

$$\eta_{b,t} = \frac{W_a (H_{a,6} - H_{a,1}) - W_{f,e} h_{c,e} + (W_{f,e} + W_{f,t}) (H'_{f,6} - H_{f,m})}{W_{f,t} h_{c,t}} \quad (6)$$

Burner-inlet velocity. - Velocity at the burner inlet was calculated from the expression for flow continuity using the static pressure measured immediately upstream of the flame holder and assuming no total-pressure or total-temperature change between the turbine outlet and the burner inlet.

$$V_5 = \frac{W_g}{\rho_5 A_5 g} = \frac{W_g R T_4}{P_5 A_5} \left(\frac{P_5}{P_4} \right)^{\frac{\gamma_4 - 1}{\gamma_4}} \quad (7)$$

Tail-pipe fuel-air ratio. - Tail-pipe fuel-air ratio is defined as the weight ratio of tail-pipe fuel flow to unburned air entering the tail-pipe burner. In obtaining the following equation, complete combustion of the engine fuel was assumed:

$$\left(\frac{f}{a} \right)_t = \frac{W_{f,t}}{3600 W_a - \frac{W_{f,e}}{0.067}} \quad (8)$$

The value of 0.067 is the stoichiometric fuel-air ratio for the fuel used.

Augmented thrust. - The augmented net thrust was calculated by subtracting the free-stream momentum of the inlet air from the jet thrust of the installation.

$$F_n = F_j - \frac{W_a}{g} V_0 \quad (9)$$

Complete free-stream total pressure recovery was assumed at the engine inlet.

The jet thrust used in this equation was determined from the balance scale measurements in the following manner:

$$F_j = B + D + D_r + \frac{W_a V_x}{g} + A_x (P_x - P_0) \quad (10)$$

The last two terms in the equation represent momentum and pressure forces on the installation at the slip joint in the inlet-air duct. The external drag of the installation D was determined over a range of test-section velocities with a blind flange installed at the engine inlet to prevent air flow through the engine. A calibrated balance piston was used to measure the drag of the exhaust-nozzle outlet rake D_r .

Standard engine thrust. - The standard engine net thrust was calculated in the same manner as the augmented net thrust.

$$F_{n,e} = F_{j,e} - \frac{W_a V_0}{g} \quad (11)$$

The jet thrust obtainable with the standard engine at rated engine speed was calculated from measurements of turbine-outlet total pressure, total temperature, and gas flow obtained during tail-pipe burning operation.

$$F_{j,e} = \frac{W_{g,4}}{g} C_j \sqrt{\frac{2\gamma_4}{\gamma_4-1} g R T_4 \left[1 - \left(\frac{P_0}{P'_6} \right)^{\frac{\gamma_4-1}{\gamma_4}} \right]} \quad (12)$$

Experimental data from previous operation of the engine indicated that the total-pressure loss across the standard-engine tail pipe between stations 4 and 6 was approximately $0.032 P_4$ at rated engine speed; therefore, $P'_6 = 0.968 P_4$. The coefficient C_j was determined from calibration of the engine with a standard tail pipe and fixed conical exhaust nozzle.

REFERENCES

1. Fleming, W. A., and Dietz, R. O.: Altitude-Wind-Tunnel Investigations of Thrust Augmentation of a Turbojet Engine. I - Performance with Tail-Pipe Burning. NACA RM E6I20, 1946.
2. Fleming, William A., and Wallner, Lewis E.: Altitude-Wind-Tunnel Investigation of Tail-Pipe Burning with a Westinghouse X24C-4B Axial-Flow Turbojet Engine. NACA RM E8J25e, 1948.
3. Conrad, E. William, and Prince, William R.: Altitude Performance and Operational Characteristics of 29-Inch-Diameter Tail-Pipe Burner with Several Fuel Systems and Flame Holders on J35 Turbojet Engine. NACA RM E9G08, 1949.
4. Thorman, H. Carl, and Campbell, Carl E.: Altitude-Wind-Tunnel Investigation of Tail-Pipe Burner with Converging Conical Burner Section on J35-A-5 Turbojet Engine. NACA RM E9I16, 1950.
5. Golladay, Richard L., and Bloomer, Harry E.: Altitude Performance and Operational Characteristics of 29-Inch-Diameter Tail-Pipe Burner with Several Fuel Systems and Fuel-Cooled Stage-Type Flame Holders on J35-A-5 Turbojet Engine. NACA RM E50A19, 1950.
6. Fleming, William A., and Golladay, Richard L.: Altitude-Wind-Tunnel Investigation of Thrust Augmentation of a Turbojet Engine. III - Performance with Tail-Pipe Burning in Standard-Size Tail Pipe. NACA RM E7F10, 1947.
7. Jansen, Emmert T., and Thorman, H. Carl: Altitude Performance Characteristics of Tail-Pipe Burner with Variable-Area Exhaust Nozzle. NACA RM E50E29, 1950.
8. Lundin, Bruce T., Dowman, Harry W., and Gabriel, David S.: Experimental Investigation of Thrust Augmentation of a Turbojet Engine at Zero Ram by Means of Tail-Pipe Burning. NACA RM E6J21, 1947.
9. Lundin, Bruce T.: Investigation of Several Clamshell Variable-Area Exhaust Nozzles for Turbojet Engines. NACA RM E9B02, 1949.
10. Turner, L. Richard, and Bogart, Donald: Constant-Pressure Combustion Charts Including Effects of Diluent Addition. NACA Rep. 937, 1949 (Formerly NACA TN's 1086 and 1655.)

TABLE I - SUMMARY OF CONFIGURATION DETAILS
 [Values of parameter under investigation indicated by braces]

Series	Con- fig- ura- tion	Combustion chamber		Flame holder			Pilot- cone diameter (in.)	Fuel system			Refer- ence figure	Exhaust- nozzle diameter (in.)	Remarks
		Diameter (in.)	Length flame- holder - leading edge to exhaust- nozzle inlet (ft-in.)	Type	Blocked area ^a (percent)	Included gutter angle (deg)		Location (in. for- ward of flame holder)	Number of spray tubes	Direction of spray			
A	A1	29	3'10 $\frac{1}{2}$ "	2-ring V	29	35	6	10 $\frac{3}{4}$	12	Side		20 $\frac{3}{32}$	Fuel-spray bars at same axial location; pilot cone 3 $\frac{3}{4}$ in. up- stream of flame holder
	A2			Sanitoroidal	19	--		10 $\frac{1}{4}$	12	Side			
	A3			Pilot cone	0	--		7	12	Side			
	A4			Fuel cooled	59	35		0	--	Forward			
B	B1	32	5'10 $\frac{1}{2}$ "	2-ring V	30	35	7	17 $\frac{1}{2}$	12	Side		25 $\frac{1}{4}$	Fuel spray bars at same axial location; pilot cone 12 in. upstream of flame holder
	B2			Radial gutter	29	35		17 $\frac{1}{2}$					
	B3			Pilot cone	0	--		5					
C	C1	32	3'10 $\frac{1}{2}$ "	2-ring V	30	20		17 $\frac{1}{2}$	12	Side		25 $\frac{5}{4}$	
	C2					35							
	C3					50							
D	D1	29	3'10 $\frac{1}{2}$ "	2-ring V	28	35		10 $\frac{3}{4}$	12	Aft	13	20 $\frac{1}{16}$	Radial fuel-spray pattern varied
	D2												
E	E1	--	4'11 $\frac{5}{8}$ "	2-ring V	28	35		20 $\frac{5}{8}$	20	Aft	14	20 $\frac{5}{32}$	Fuel-spray pattern varied; converging combustion chamber
	E2	--						25 $\frac{5}{8}$					
	E3	--											
F	F1	29	3'10 $\frac{1}{2}$ "	2-ring V	25	35		10 $\frac{3}{4}$	12	Aft		20 $\frac{3}{32}$	
	F2									Side			
	F3									Forward			
G	G1	32	3'10 $\frac{1}{2}$ "	2-ring V	30	35		17 $\frac{1}{2}$	12	Side		25 $\frac{3}{4}$	
	G2							25 $\frac{1}{2}$					
H	H1	29	3'10 $\frac{1}{2}$ "	2-ring V	29	35		10 $\frac{3}{4}$	12	Aft		20 $\frac{5}{32}$	
	H2	34			28			17 $\frac{1}{2}$		Side		25 $\frac{5}{32}$	
	H3	32			30								
	H4	29			27								
I	I1	32	1'10 $\frac{1}{2}$ "	2-ring V	30	35		17 $\frac{1}{2}$	12	Side		25 $\frac{5}{32}$	
	I2		3'10 $\frac{1}{2}$ "										
	I3		5'10 $\frac{1}{2}$ "										
J	J1	32	4'8"	2-ring V	30	35		27 $\frac{1}{2}$	12	Side		Variable	

^aBased on combustion-chamber cross-sectional area.

^bFlame holder mounted in diffuser.

^cConical spray nozzles.

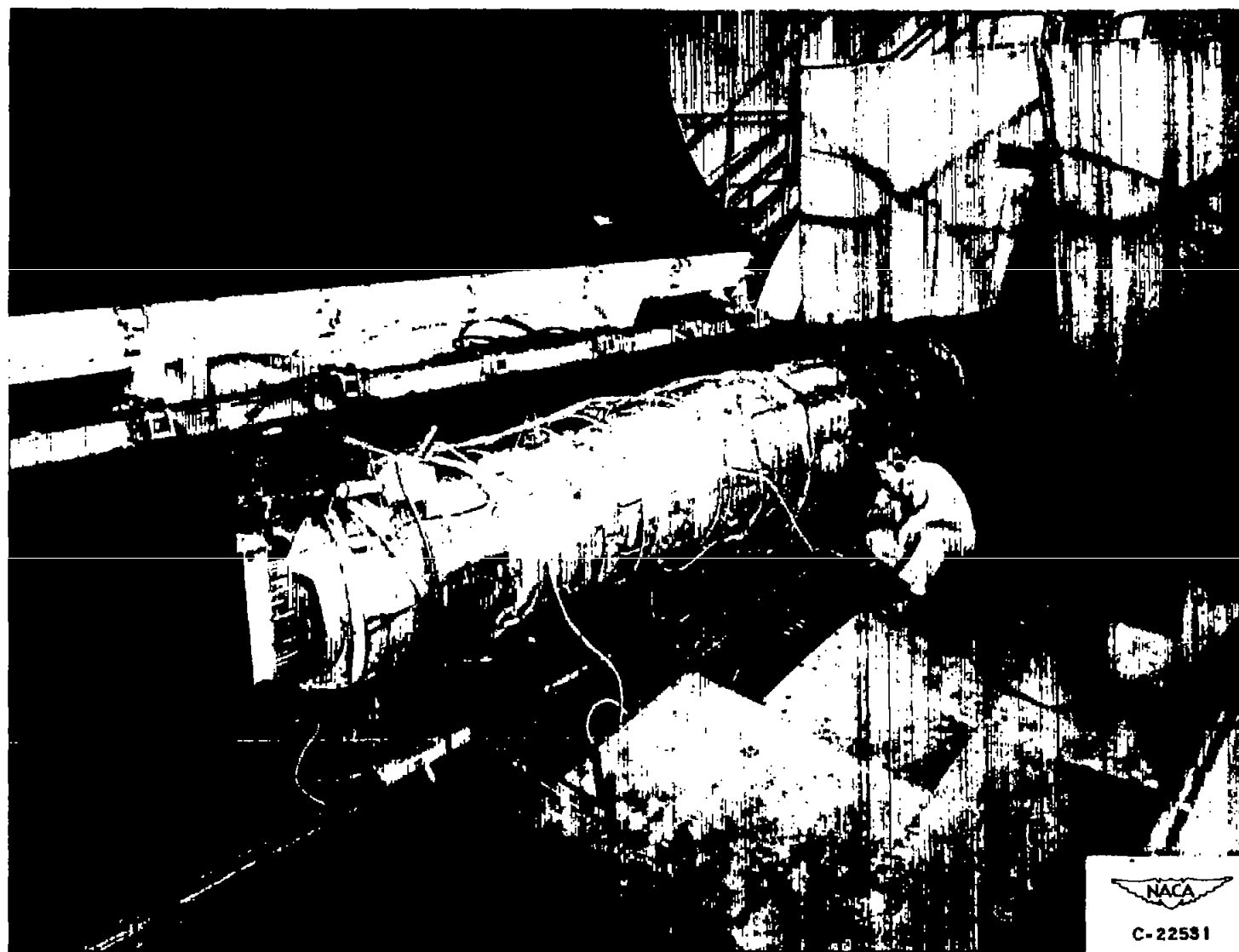


Figure 1. - Typical installation of engine with tail-pipe burner in altitude wind tunnel.

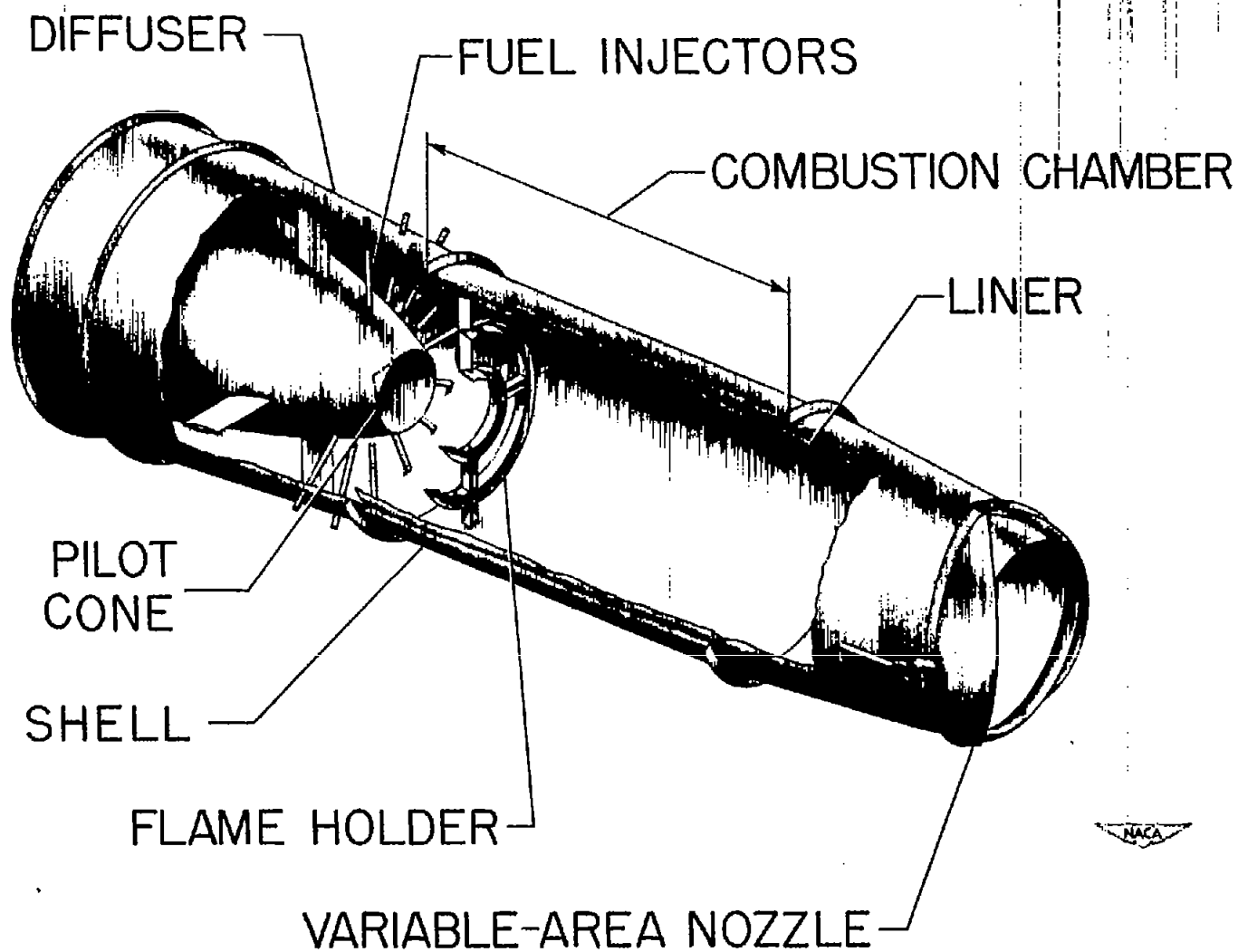
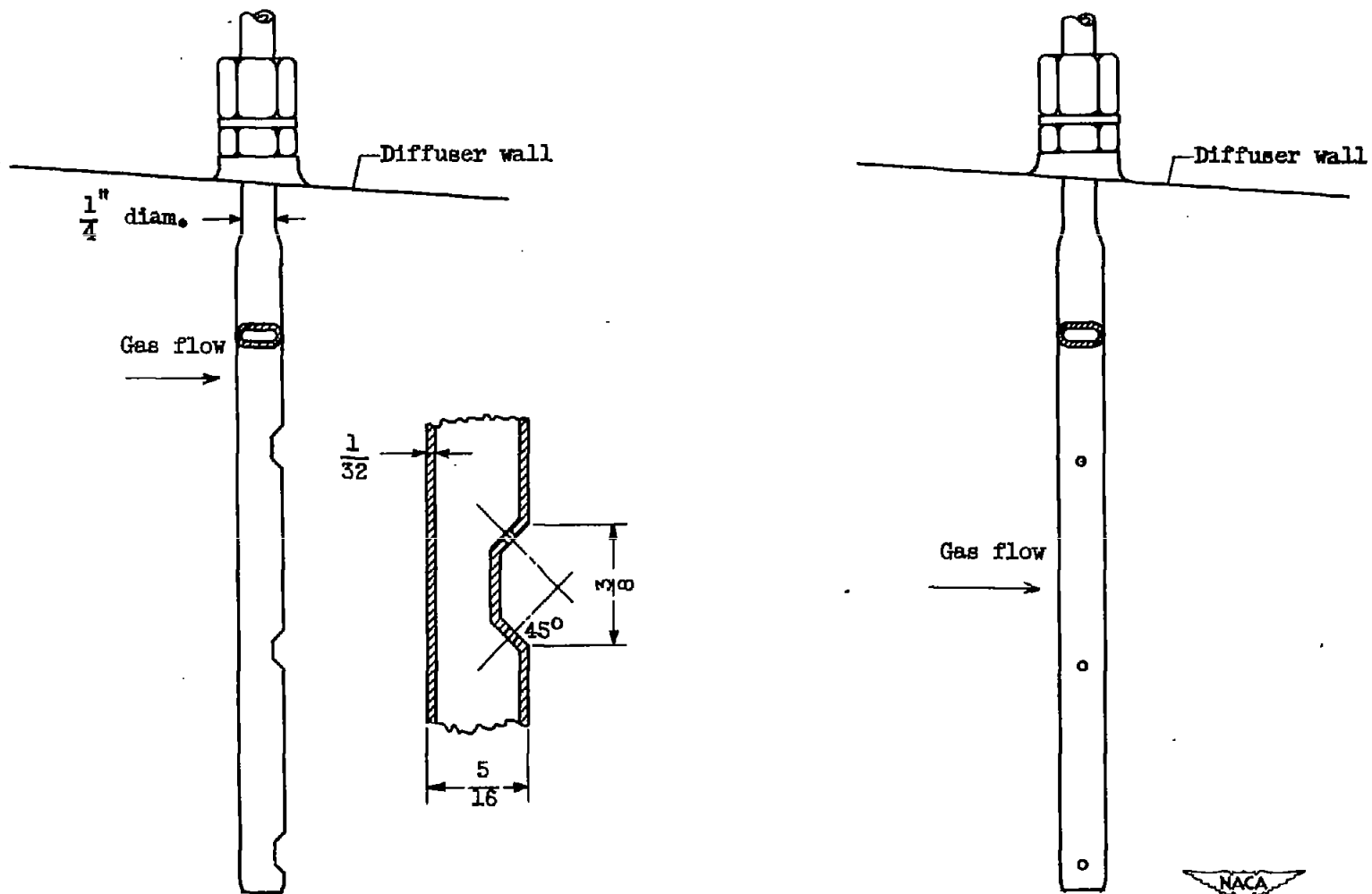


Figure 2. - Cutaway view of a typical tail-pipe burner.

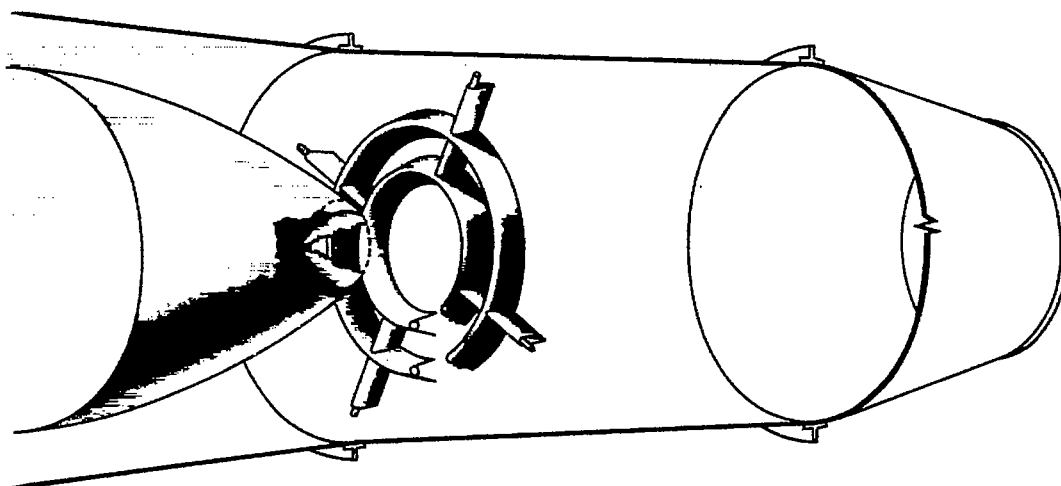


(a) Impinging jets.

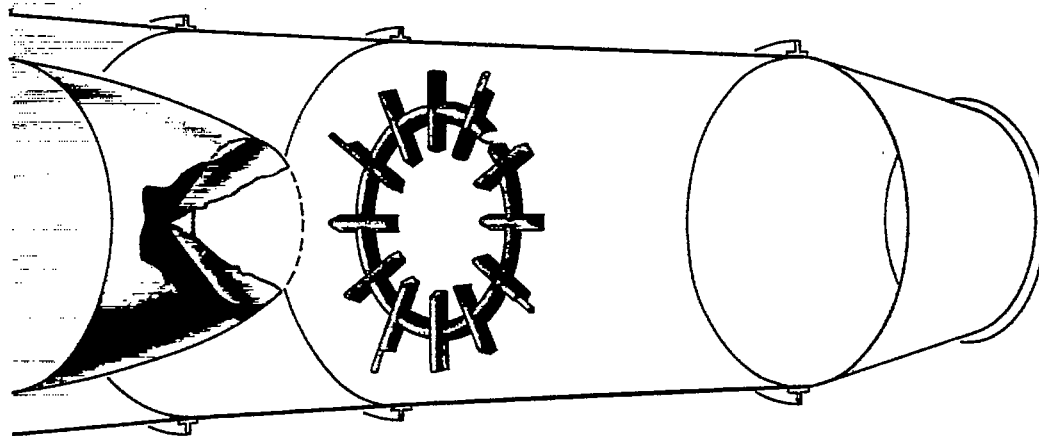
(b) Side spray.

Figure 3. - Details of fuel-injector tubes.

2058



(a) Two-ring V-gutter flame holder.

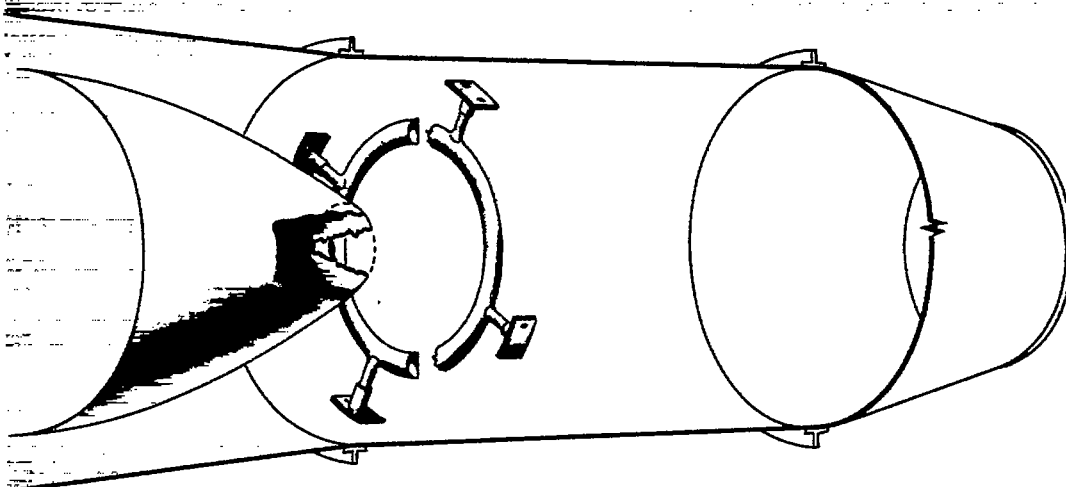


(b) Radial gutter flame holder.

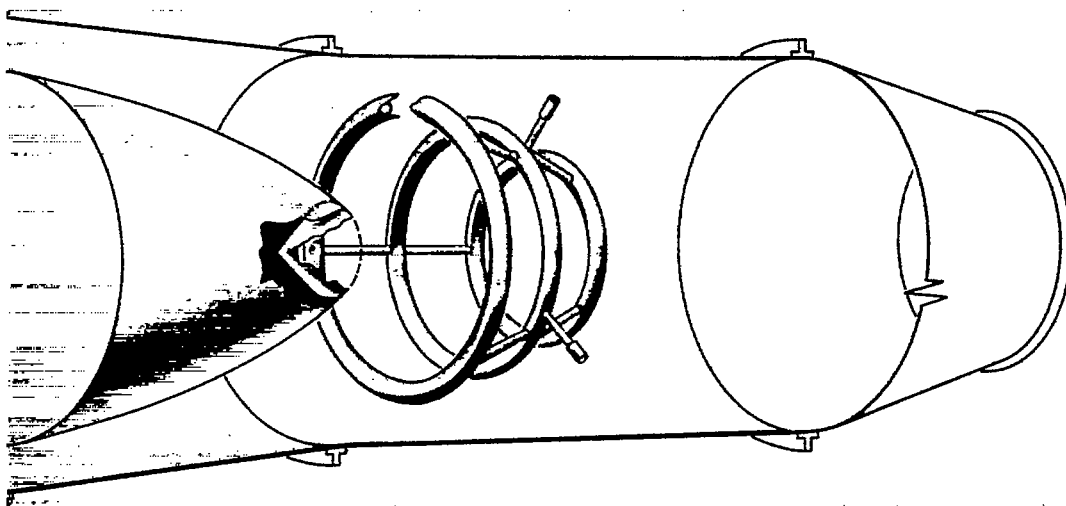
Figure 4. - Flame-holder types investigated.



206 1132 1131



(c) Semitoroidal flame holder.



(d) Fuel-cooled flame holder.

Figure 4. - Concluded. Flame-holder types investigated.



2058

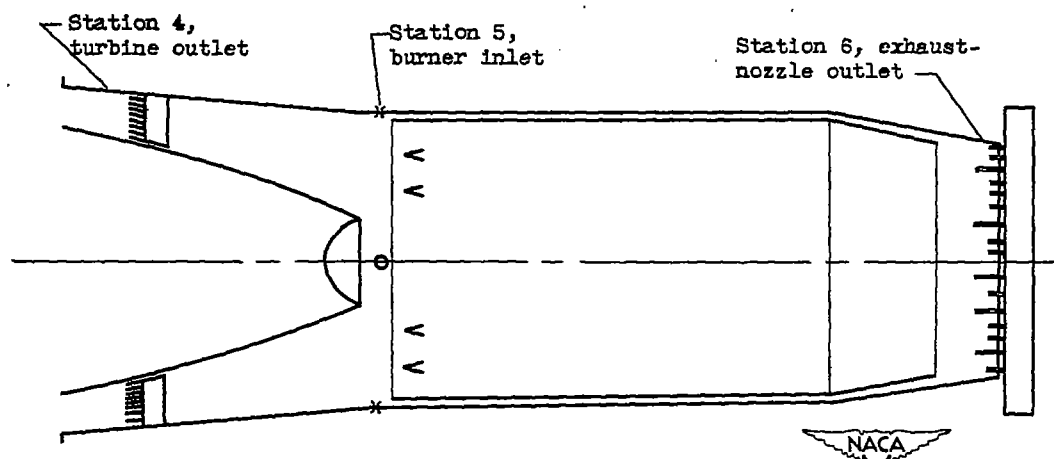
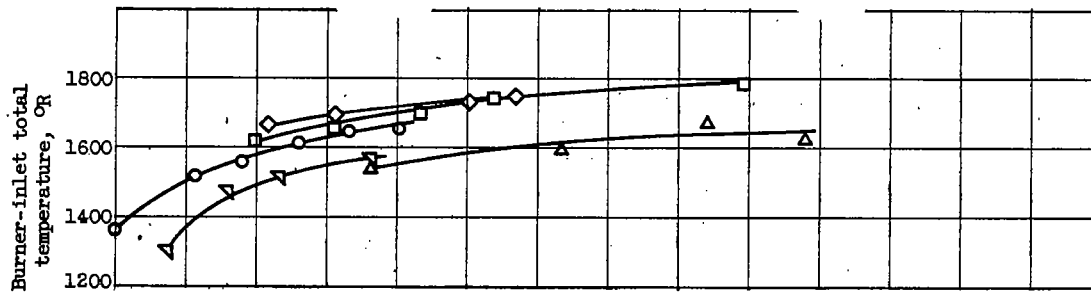
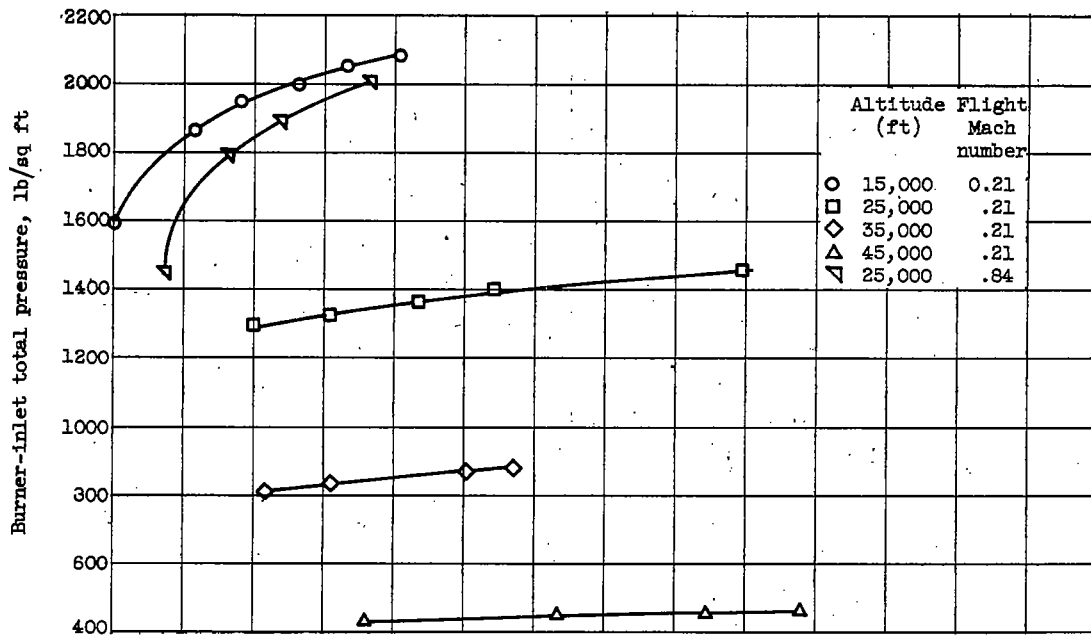


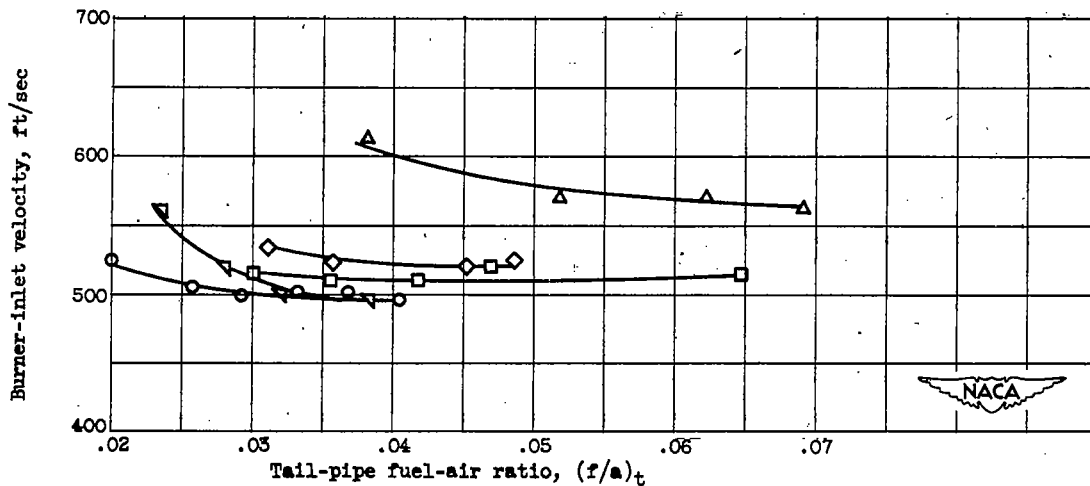
Figure 5. - Location of tail-pipe-burner instrumentation.



(a) Burner-inlet total temperature.

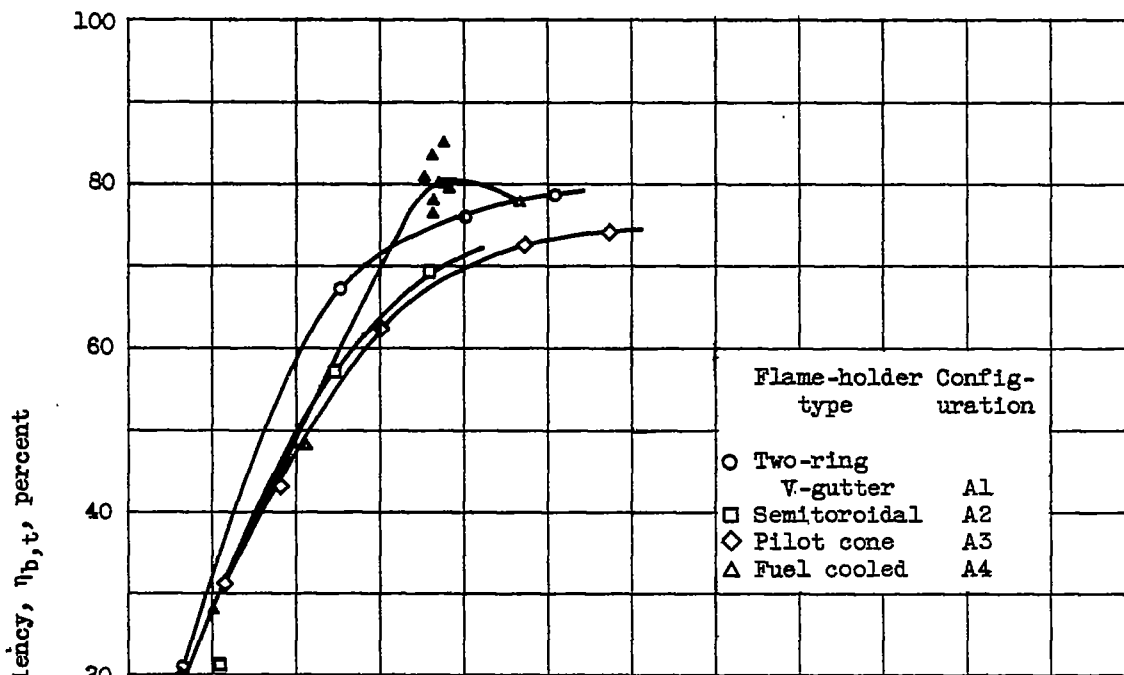


(b) Burner-inlet total pressure.

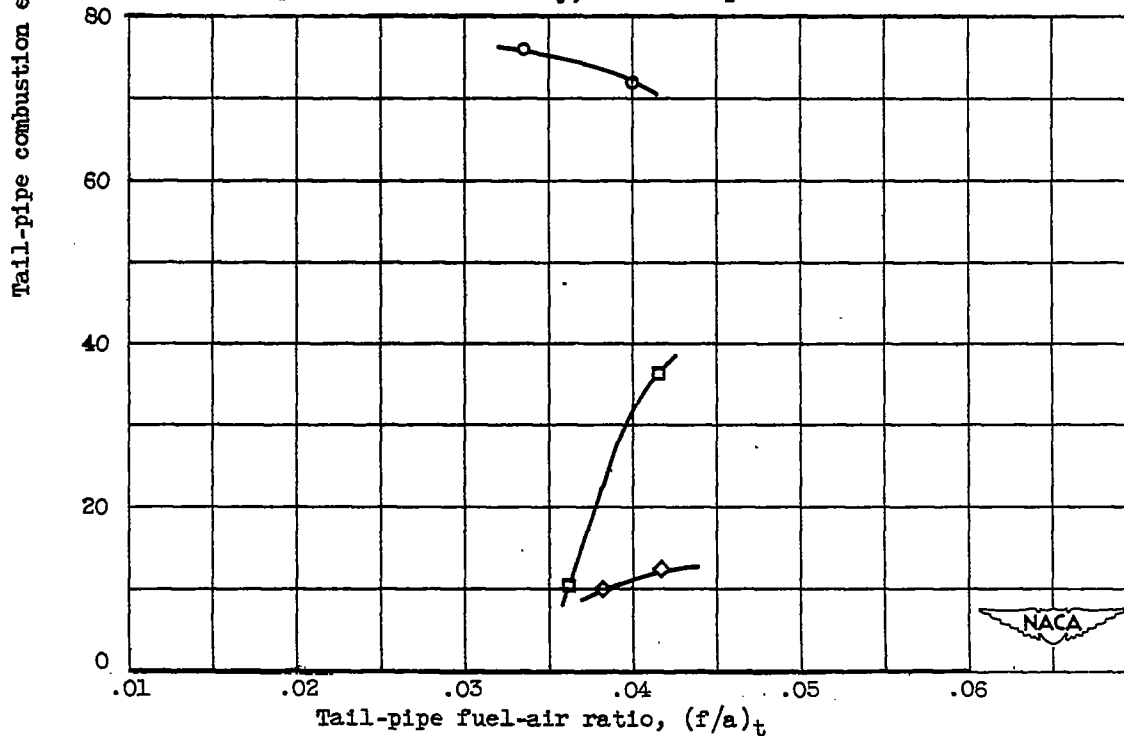


(c) Burner-inlet velocity.

Figure 6. - Typical effect of tail-pipe fuel-air ratio on burner-inlet conditions. Fixed-area exhaust nozzle.

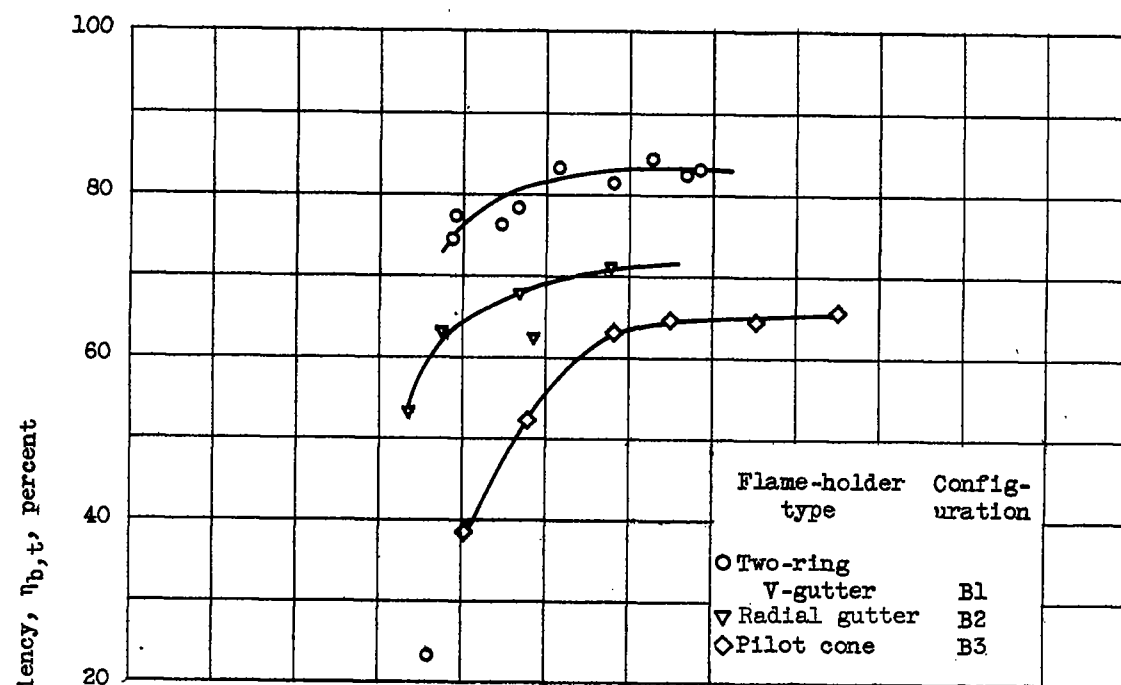


(a) Burner-inlet total pressure, 2500 to 3400 pounds per square foot;
burner-inlet velocity, 420 feet per second.

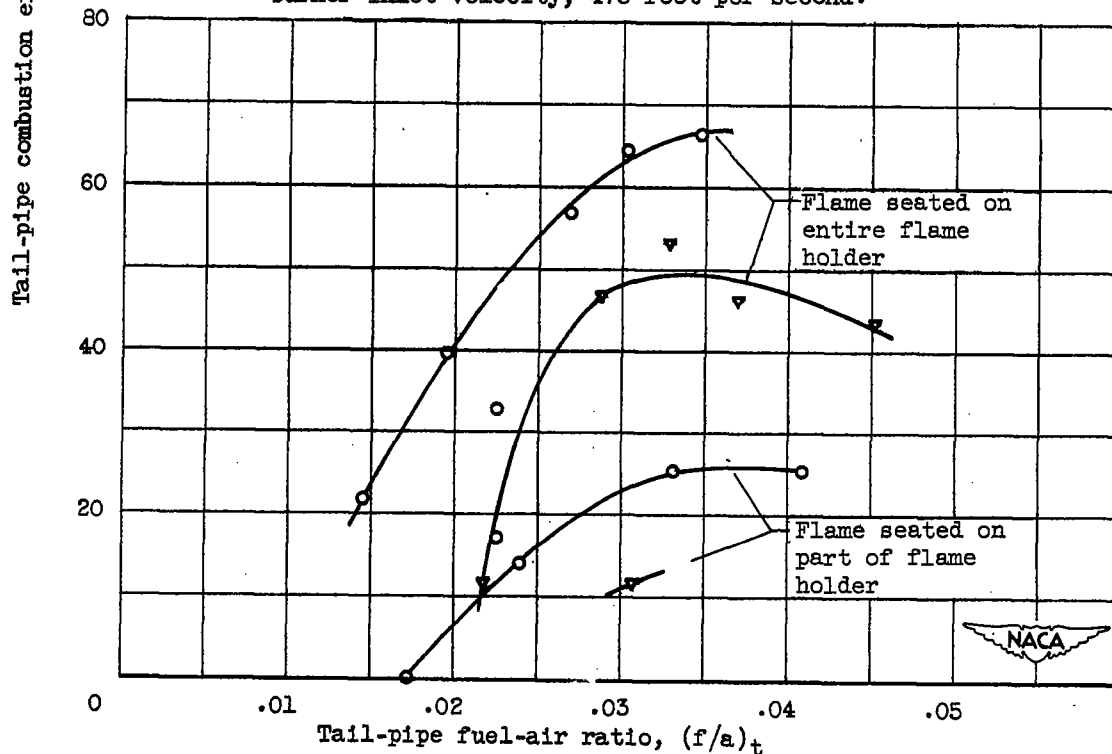


(b) Burner-inlet total pressure, 400 to 600 pounds per square foot;
burner-inlet velocity, 420 feet per second.

Figure 7. - Effect of flame-holder design on tail-pipe combustion efficiency.
Small pilot cone.



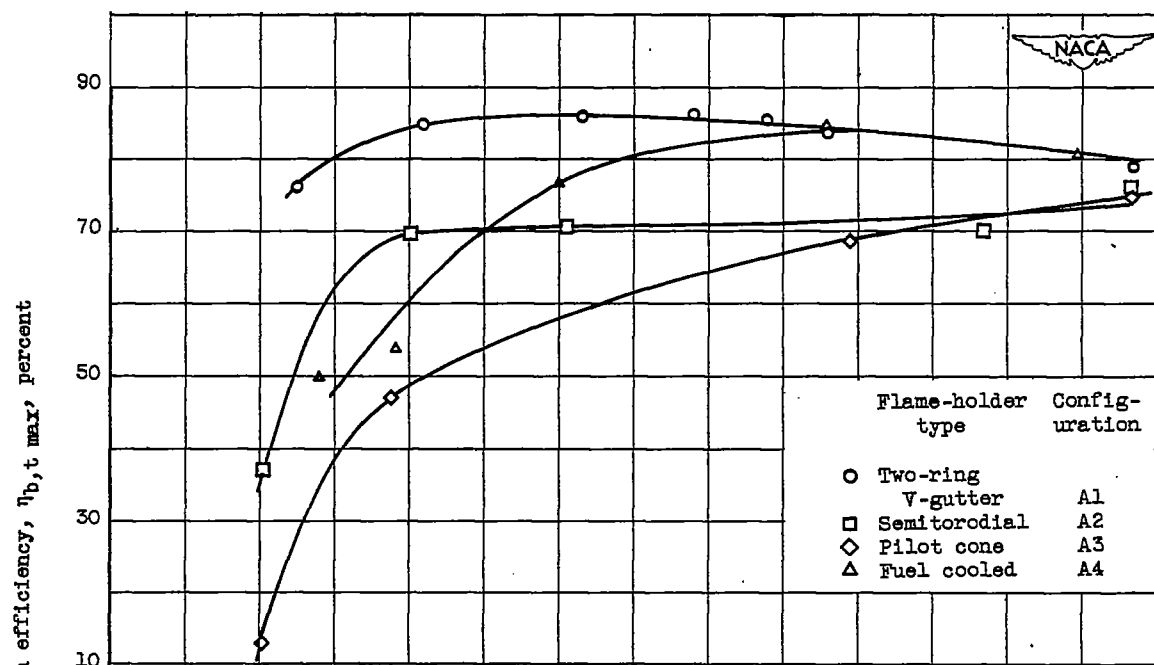
(a) Burner-inlet total pressure, 1275 to 1400 pounds per square foot; burner-inlet velocity, 475 feet per second.



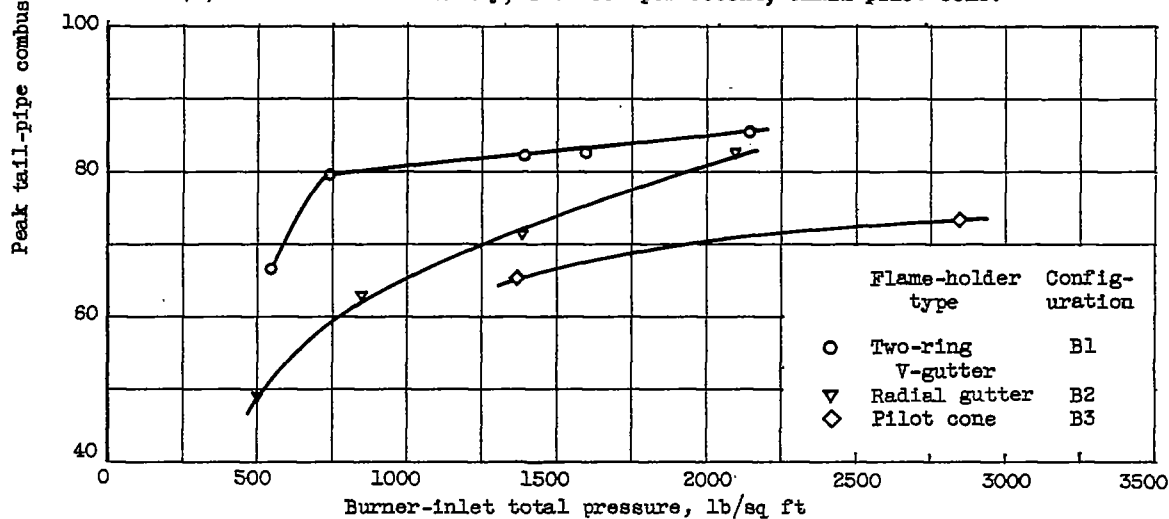
(b) Burner-inlet total pressure, 425 to 525 pounds per square foot; burner-inlet velocity, 515 feet per second.

Figure 8. - Effect of flame-holder design on tail-pipe combustion efficiency. Large pilot cone.

2058

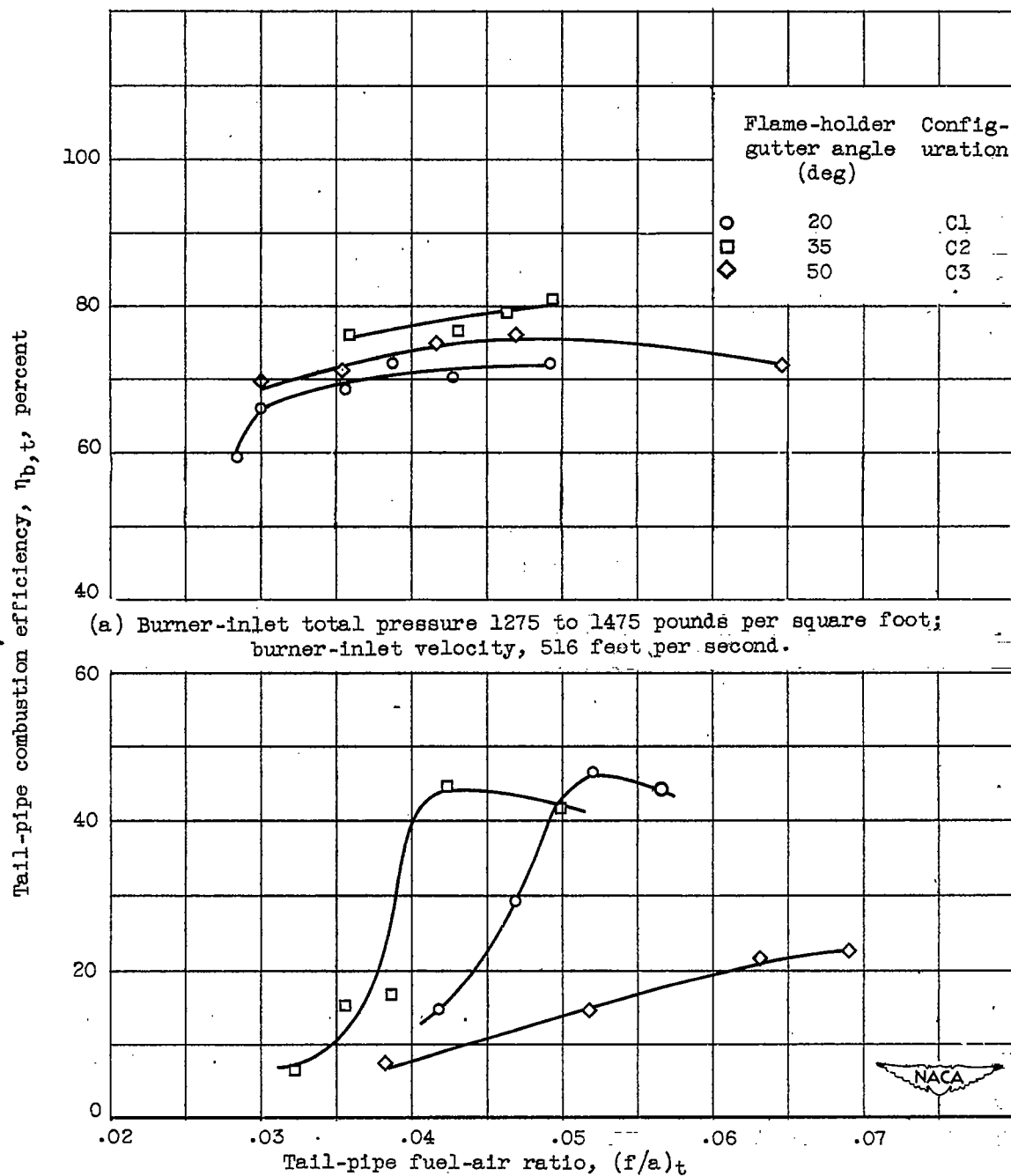


(a) Burner-inlet velocity, 420 feet per second; small pilot cone.



(b) Burner-inlet velocity, 475 to 515 feet per second; large pilot cone.

Figure 9. - Variation of peak tail-pipe combustion efficiency with burner-inlet total pressure for various flame-holder types.



(a) Burner-inlet total pressure 1275 to 1475 pounds per square foot;
burner-inlet velocity, 516 feet per second.

(b) Burner-inlet total pressure, 425 to 525 pounds per square foot;
burner-inlet velocity, 560 feet per second.

Figure 10. - Effect of included gutter angle on tail-pipe combustion efficiency.
Two-ring V-gutter flame holders.

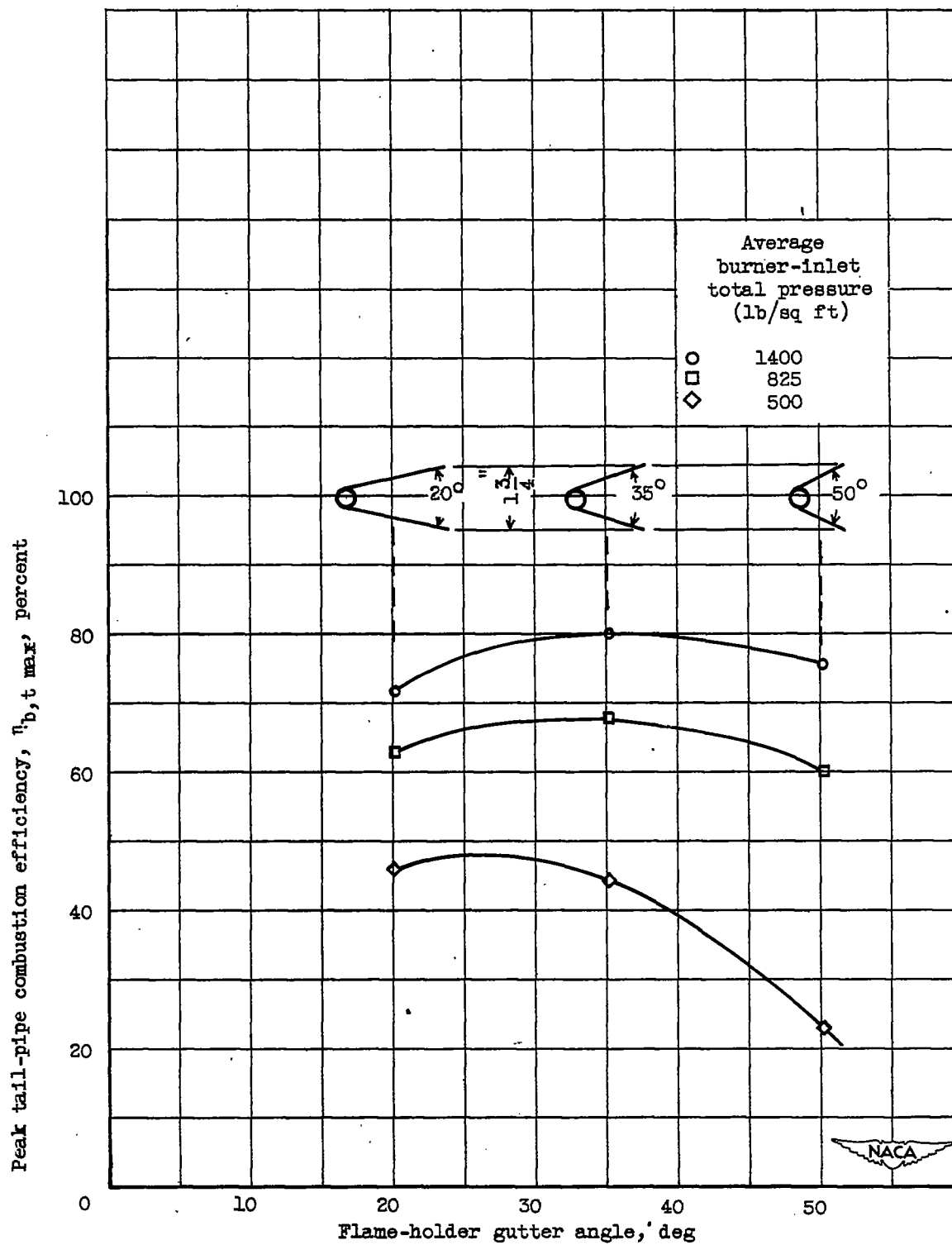


Figure 11. - Variation of peak tail-pipe combustion efficiency with flame-holder gutter angle. Two-ring V-gutter flame holders.

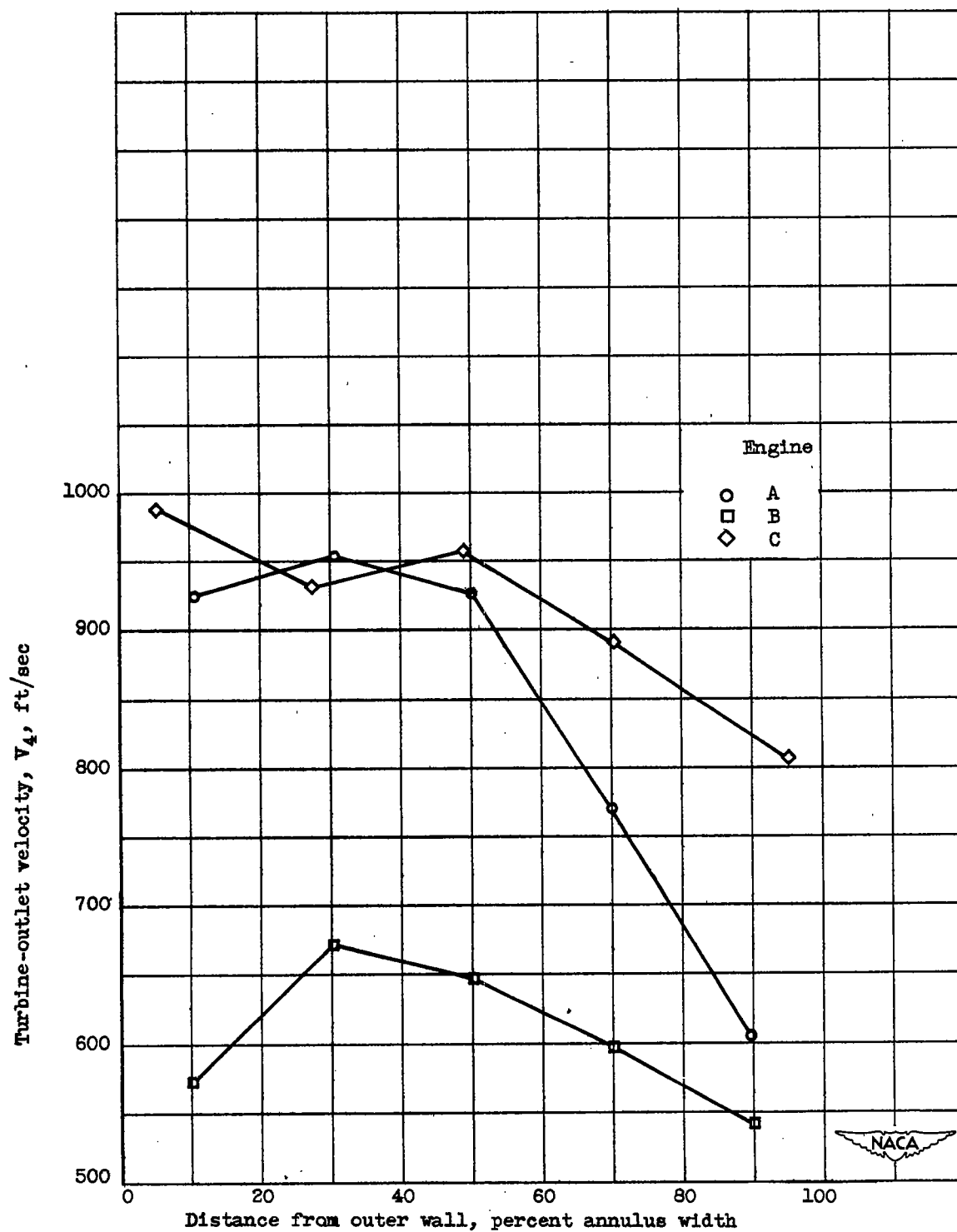
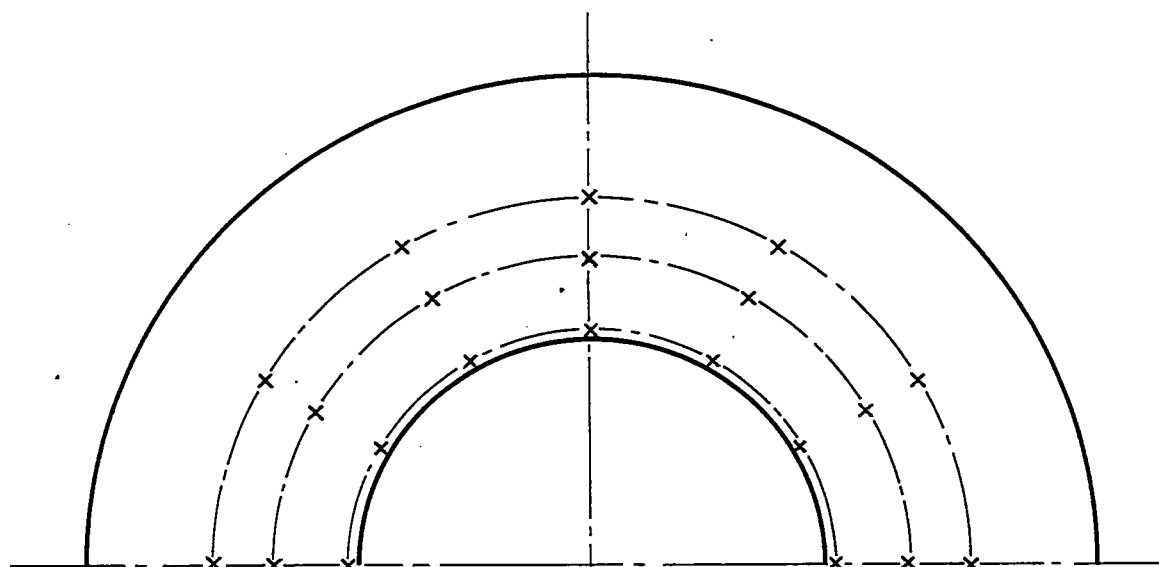
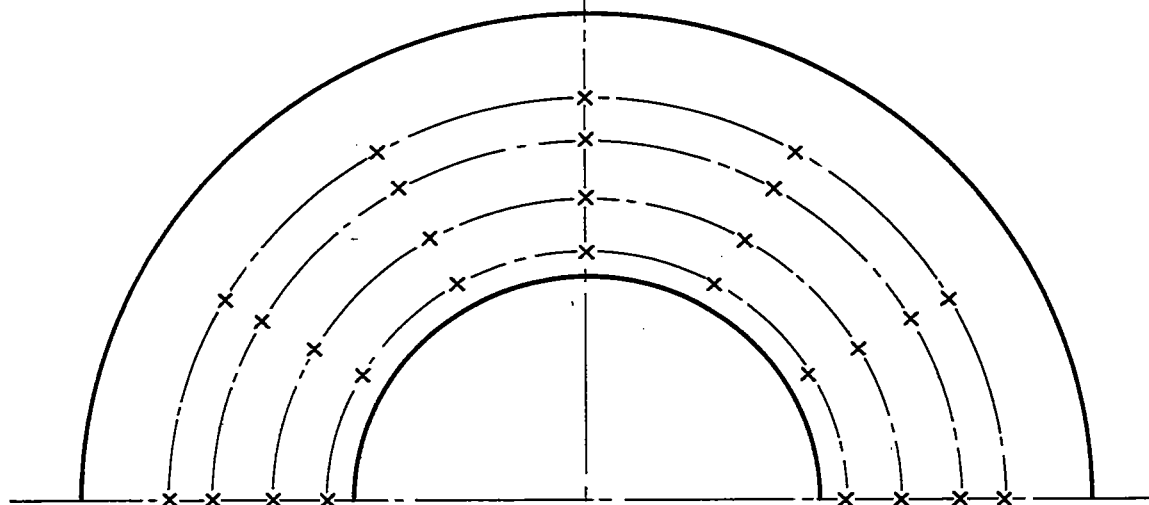


Figure 12. - Typical velocity profiles approximately 6 inches downstream of turbine.



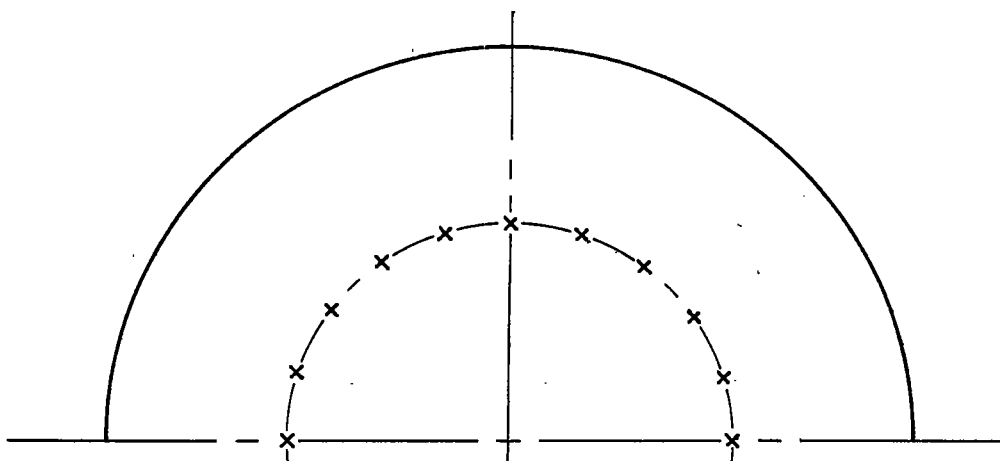
(a) Locations of radial-spray-tube orifices, configuration D1.



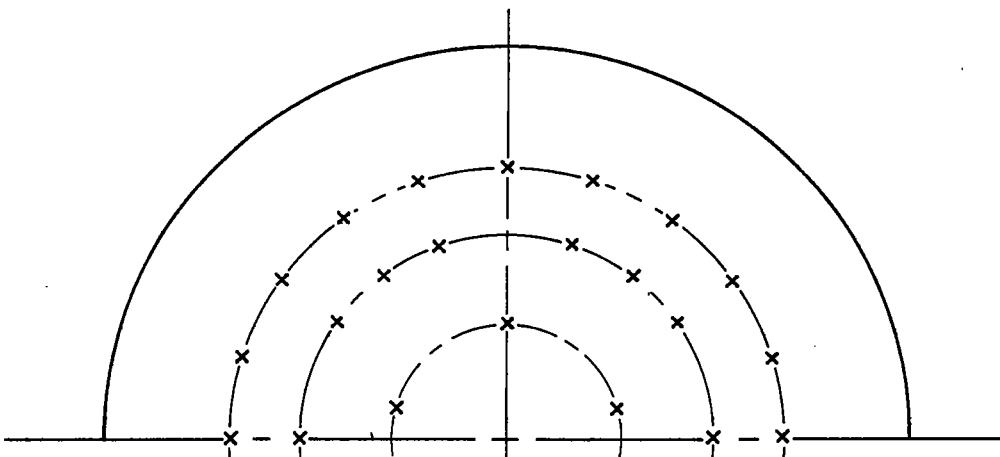
(b) Locations of radial-spray-tube orifices, configuration D2.



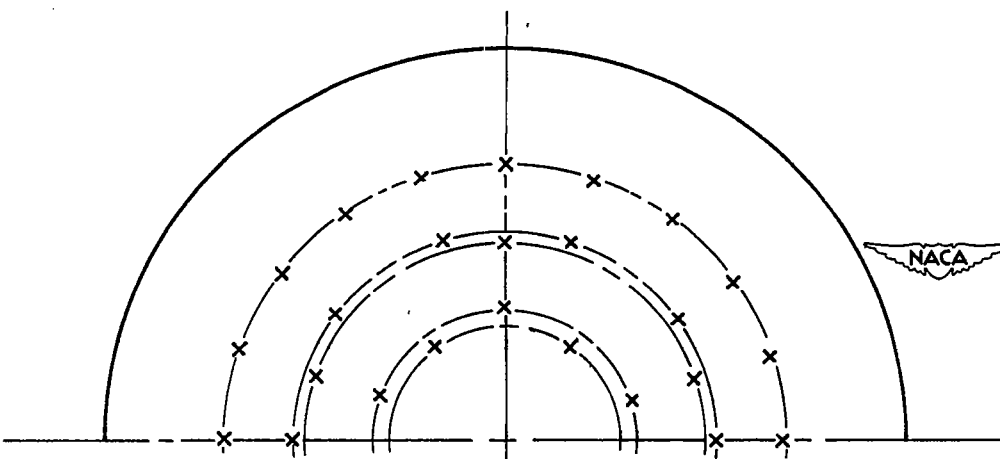
Figure 13. - Fuel patterns used with configurations D1 and D2.



(a) Locations of conical spray nozzles, configuration E1.

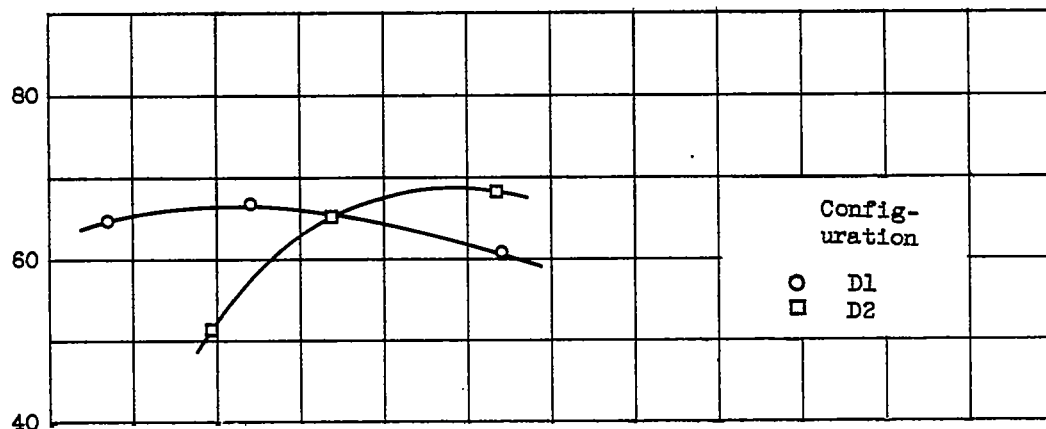


(b) Locations of radial-spray-tube orifices, configuration E2.

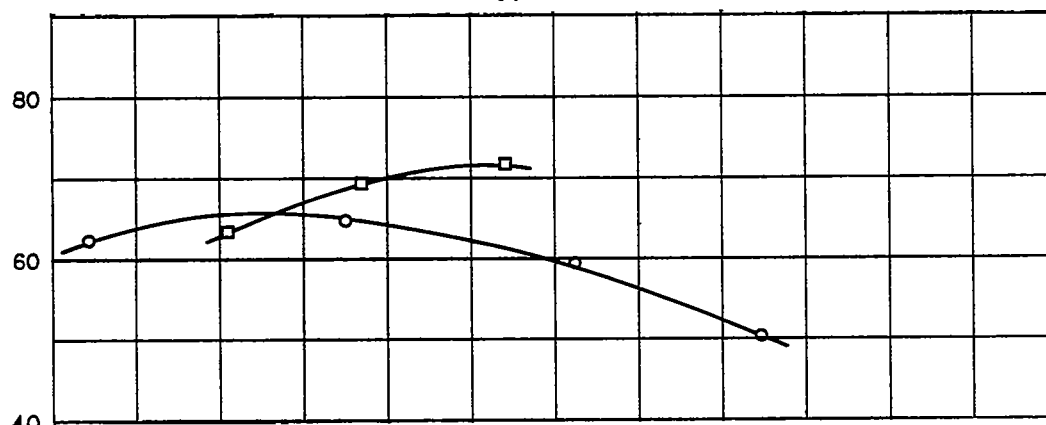


(c) Locations of radial-spray-tube orifices, configuration E3.

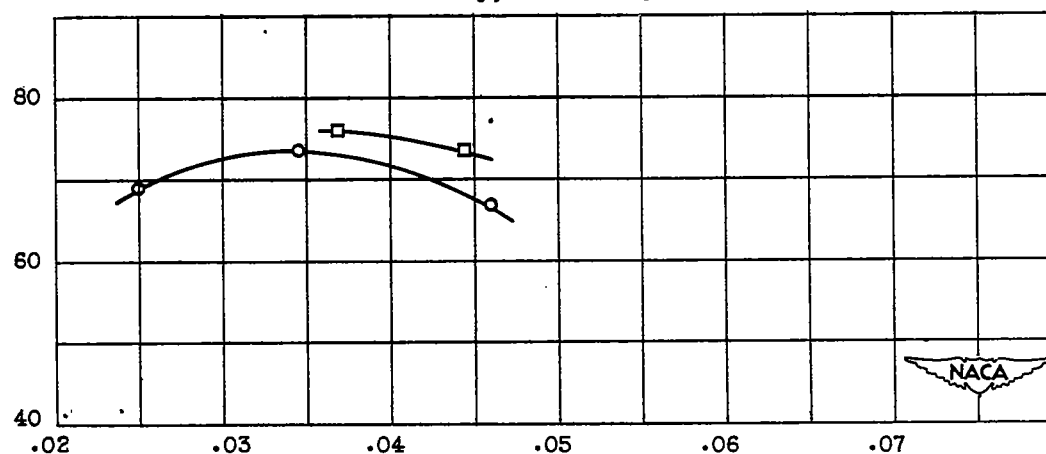
Figure 14. - Fuel patterns used with configurations E1, E2, and E3.



(a) Burner-inlet total pressure, 880 to 1080 pounds per square foot;
burner-inlet velocity, 430 feet per second.



(b) Burner-inlet total pressure, 1400 to 1700 pounds per square foot;
burner-inlet velocity, 430 feet per second.

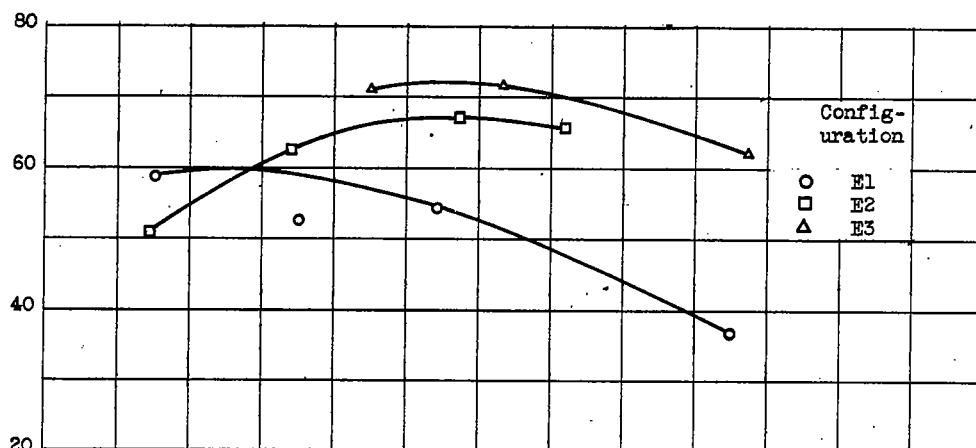


(c) Burner-inlet total pressure, 3000 to 3500 pounds per square foot;
burner-inlet velocity, 430 feet per second.

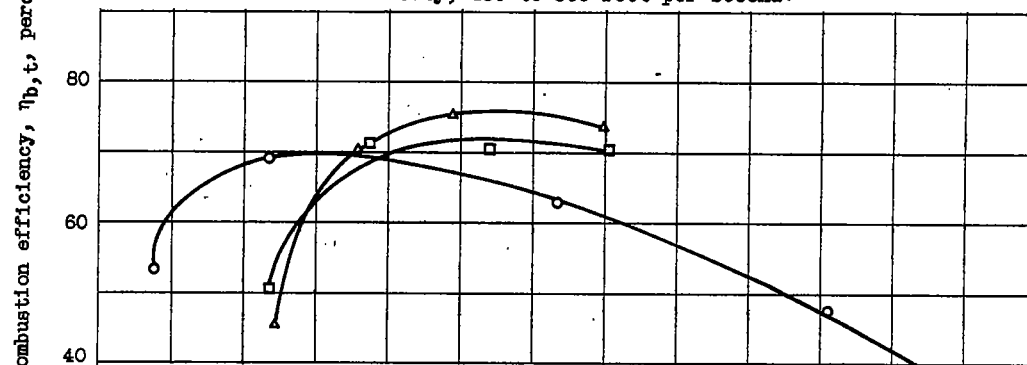
Figure 15. - Effect of radial fuel distribution on tail-pipe combustion efficiency.
Series D configurations (fig. 13).

CONFIDENTIAL

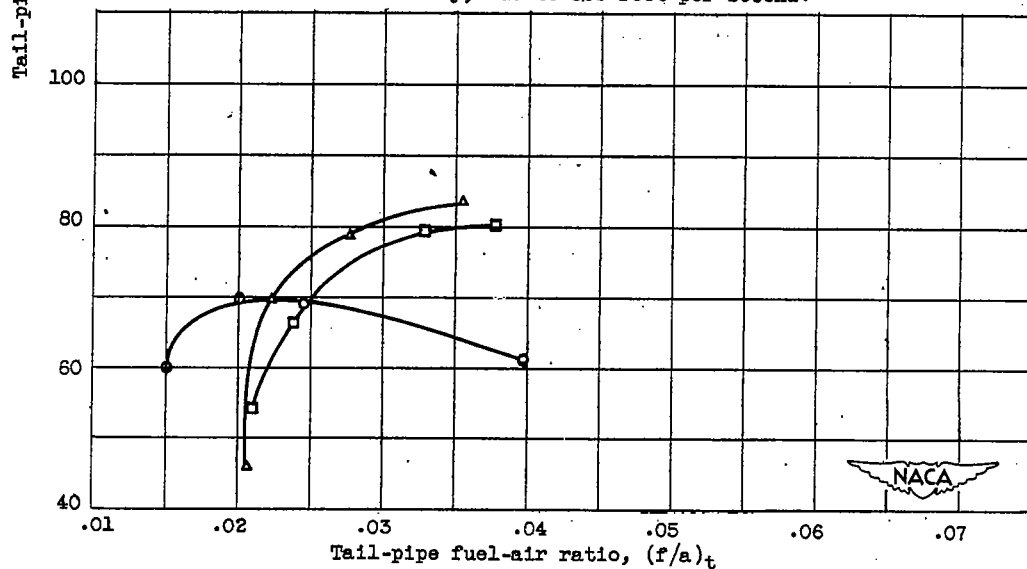
NACA RM E50K22



(a) Burner-inlet total pressure, 825 to 1065 pounds per square foot;
burner-inlet velocity, 450 to 500 feet per second.



(b) Burner-inlet total pressure, 1300 to 2500 pounds per square foot;
burner-inlet velocity, 450 to 500 feet per second.



(c) Burner-inlet total pressure, 2900 to 3500 pounds per square foot;
burner-inlet velocity, 450 to 500 feet per second.

Figure 16. - Effect of radial fuel distribution on tail-pipe combustion efficiency.
Series E configurations (fig. 14).

CONFIDENTIAL

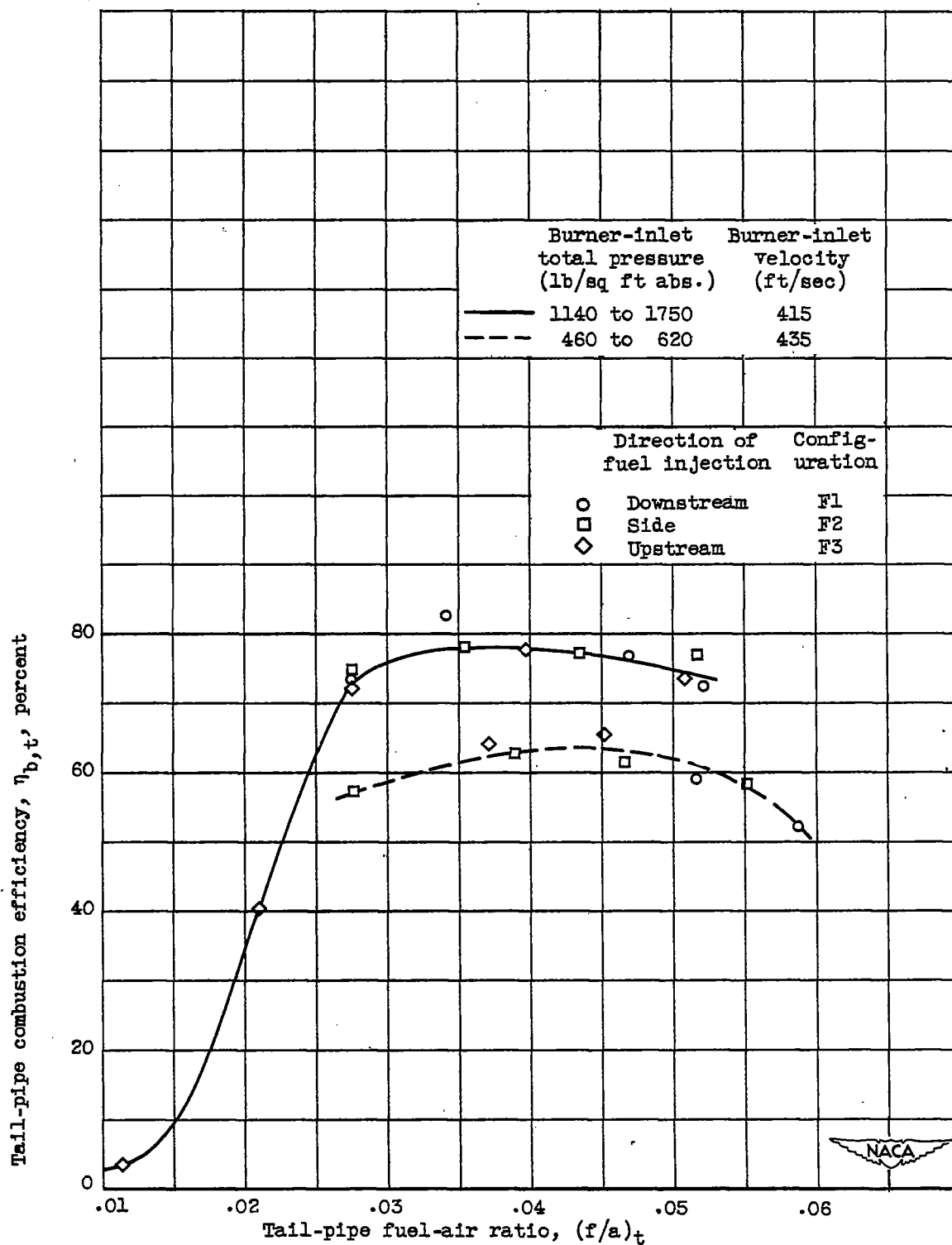
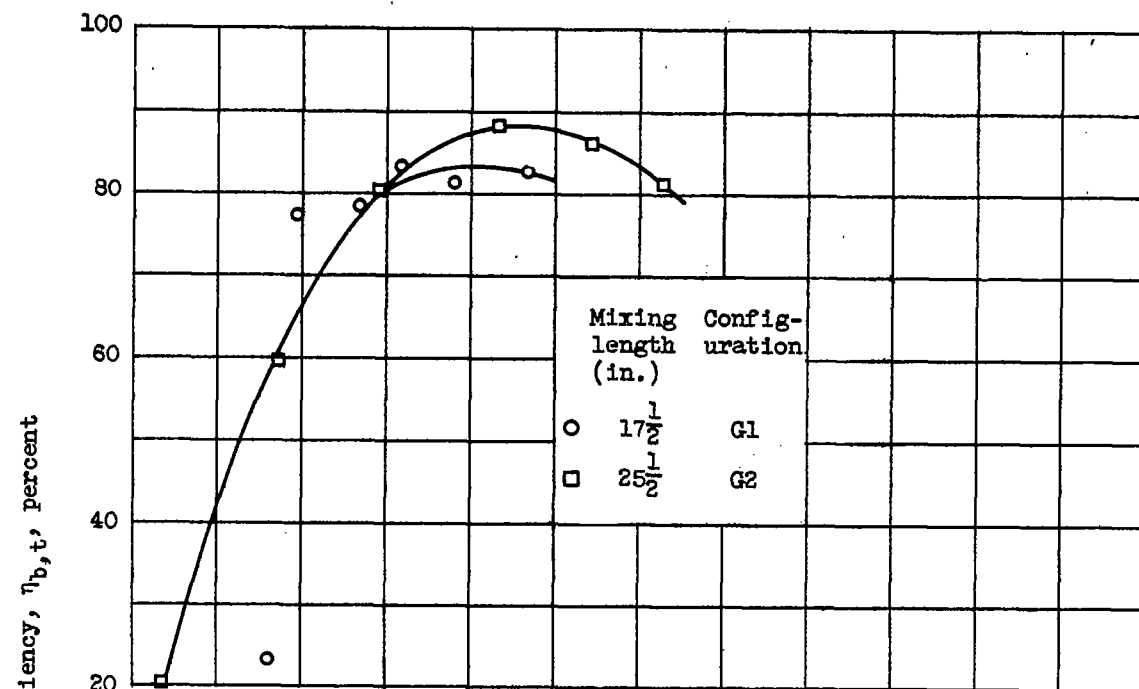
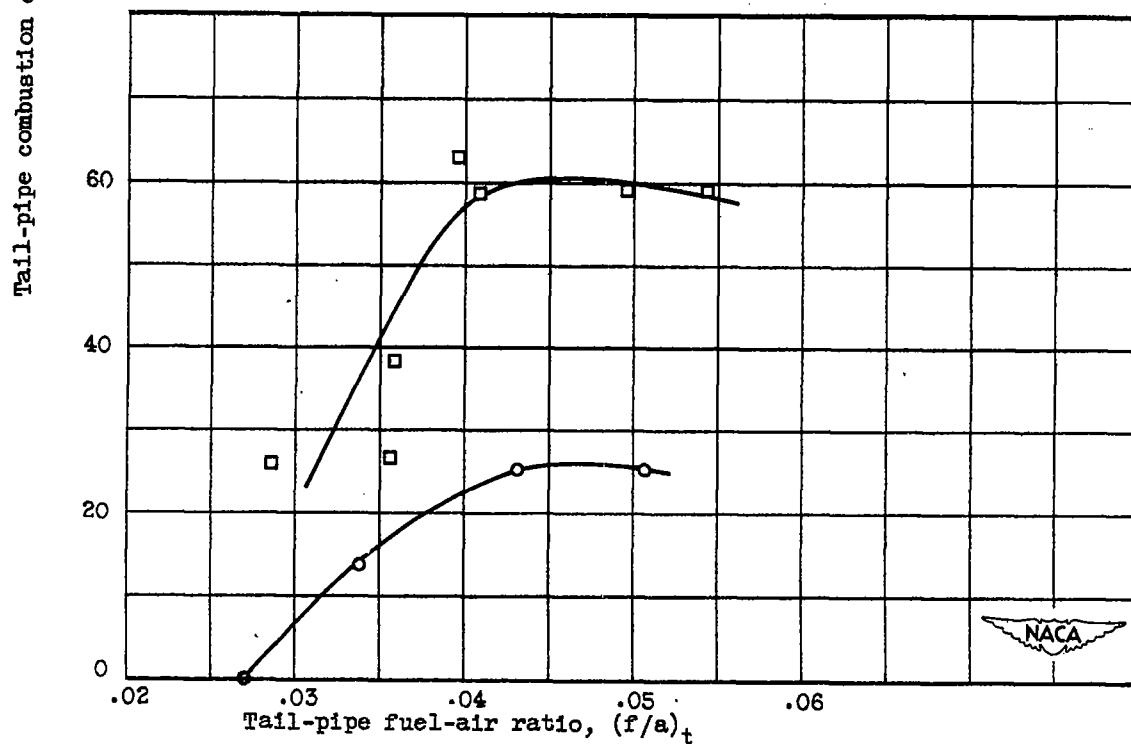


Figure 17. - Effect of direction of fuel injection on tail-pipe combustion efficiency.

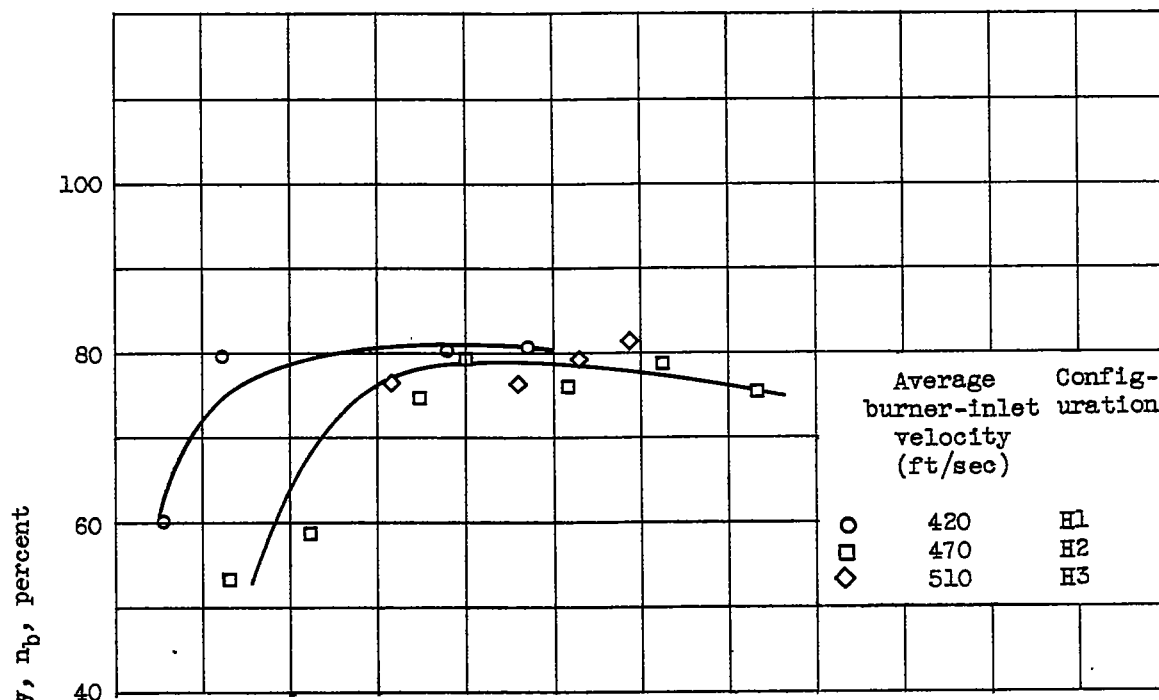


(a) Burner-inlet total pressure, 1200 to 1425 pounds per square foot;
burner-inlet velocity, 470 feet per second.

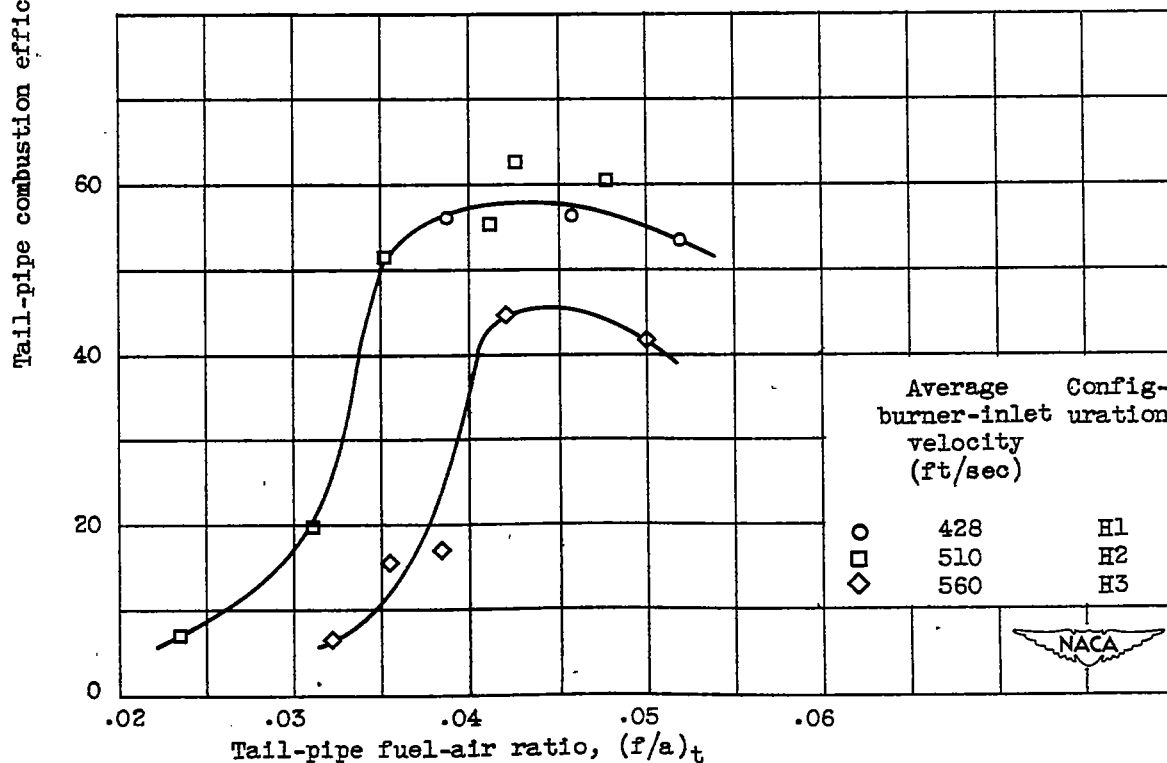


(b) Burner-inlet total pressure, 450 to 525 pounds per square foot;
burner-inlet velocity, 525 feet per second.

Figure 18. - Effect of fuel mixing length on tail-pipe combustion efficiency.

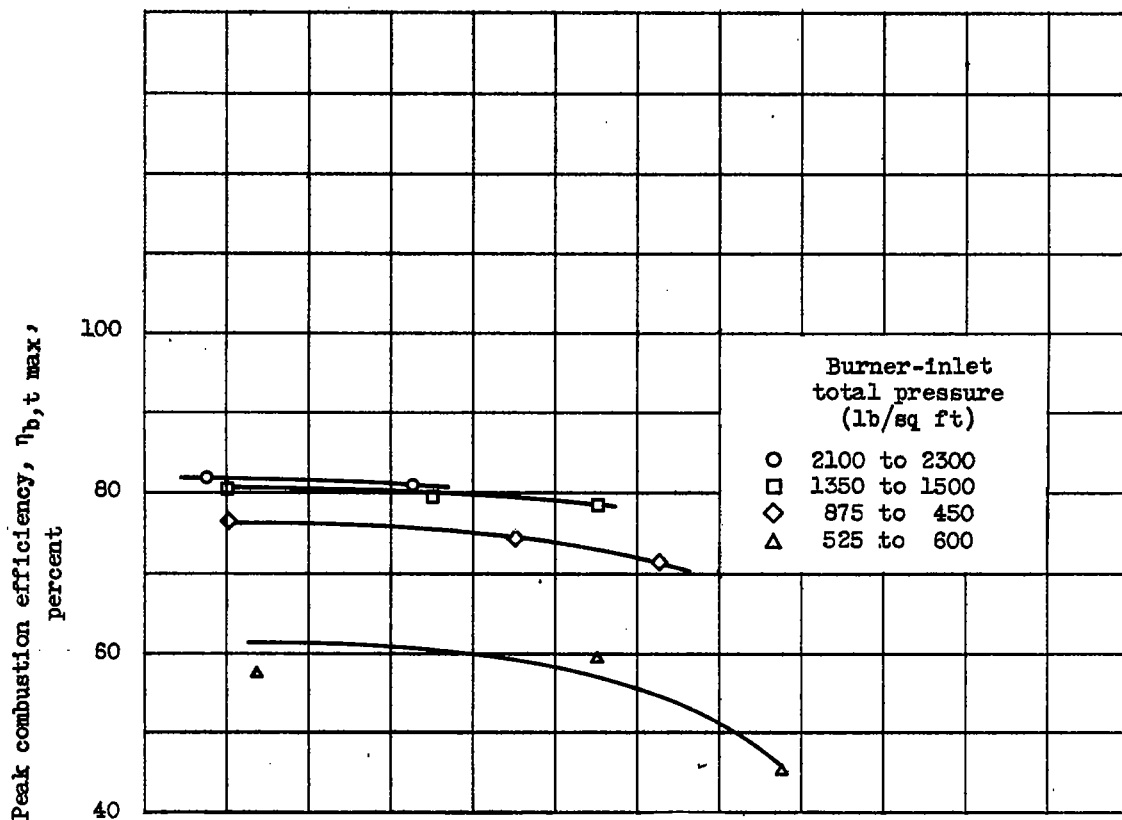


(a) Burner-inlet total pressure, 1200 to 1600 pounds per square foot.

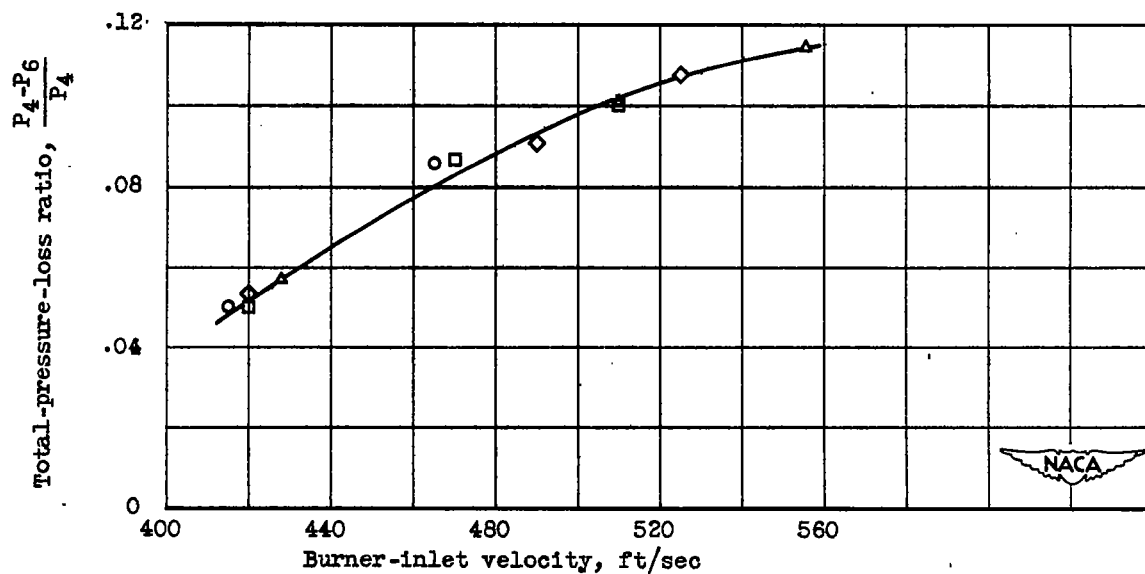


(b) Burner-inlet total pressure, 425 to 605 pounds per square foot.

Figure 19. - Effect of burner-inlet velocity on tail-pipe combustion efficiency.

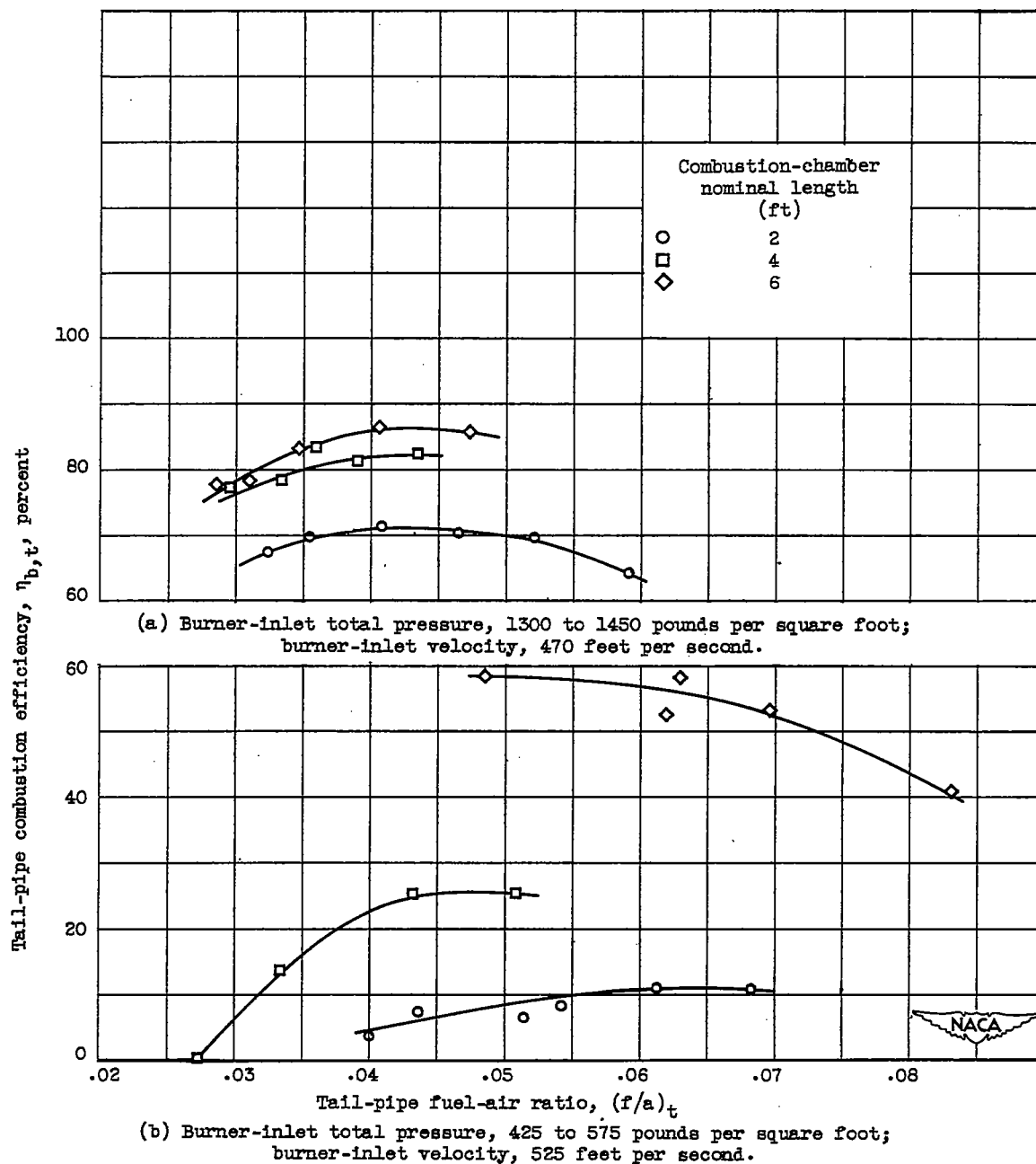


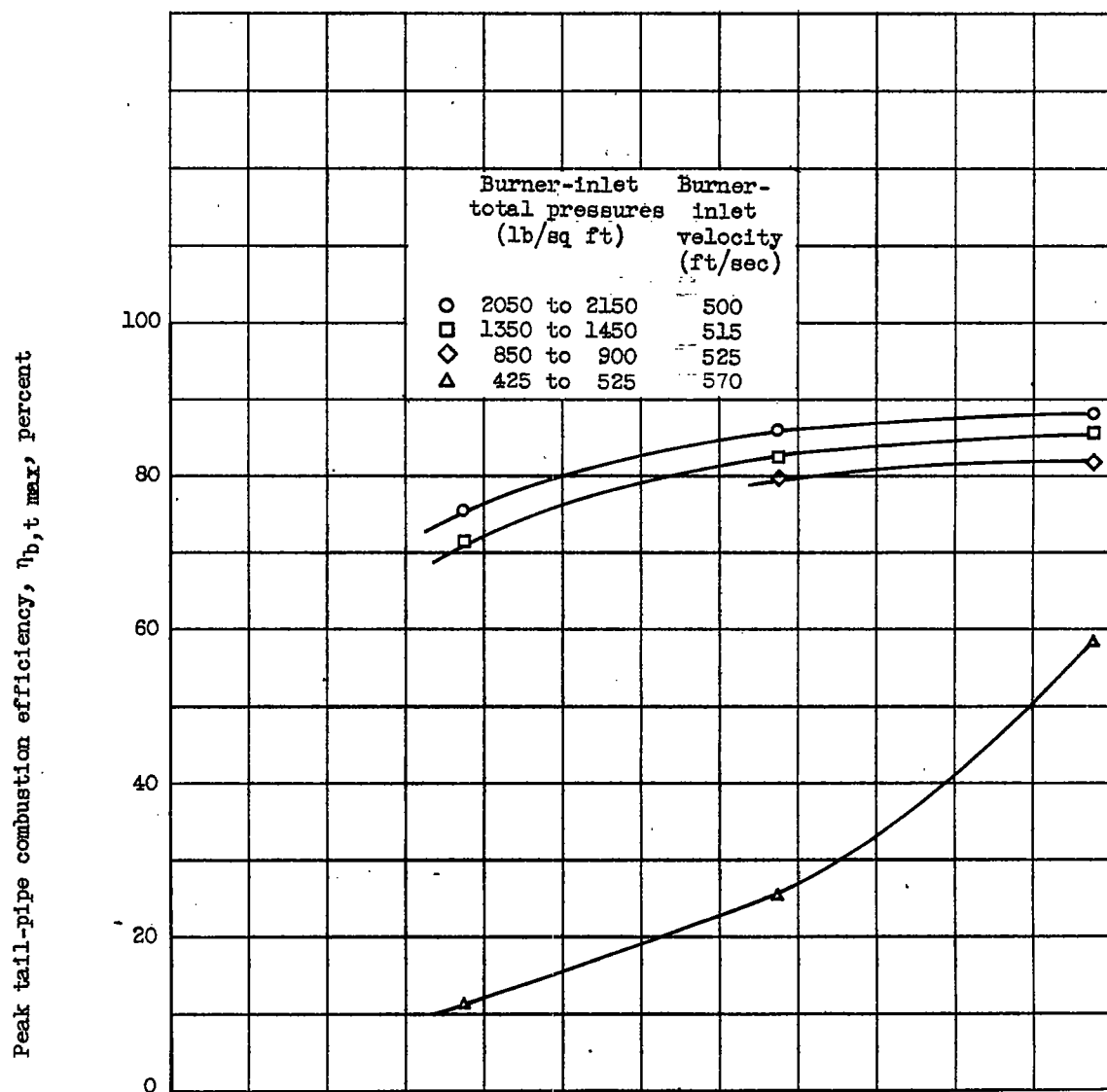
(a) Peak tail-pipe combustion efficiency.



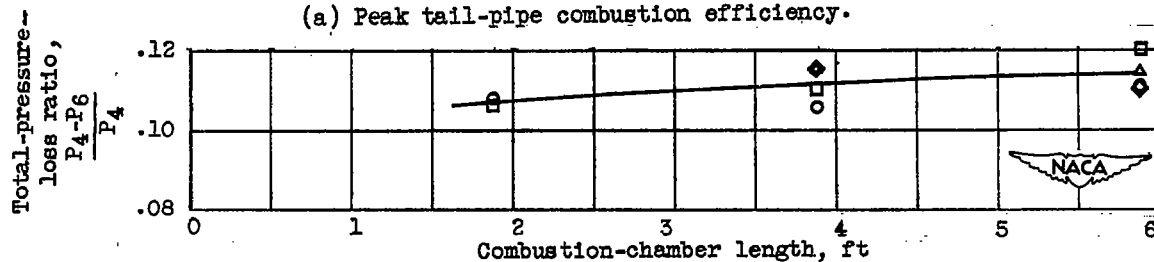
(b) Total-pressure-loss ratio.

Figure 20. - Effect of burner-inlet velocity on peak tail-pipe combustion efficiency and total-pressure-loss ratio.





(a) Peak tail-pipe combustion efficiency.



(b) Total-pressure-loss ratio.

Figure 22. - Effect of combustion-chamber length on peak tail-pipe combustion efficiency and total-pressure-loss ratio.

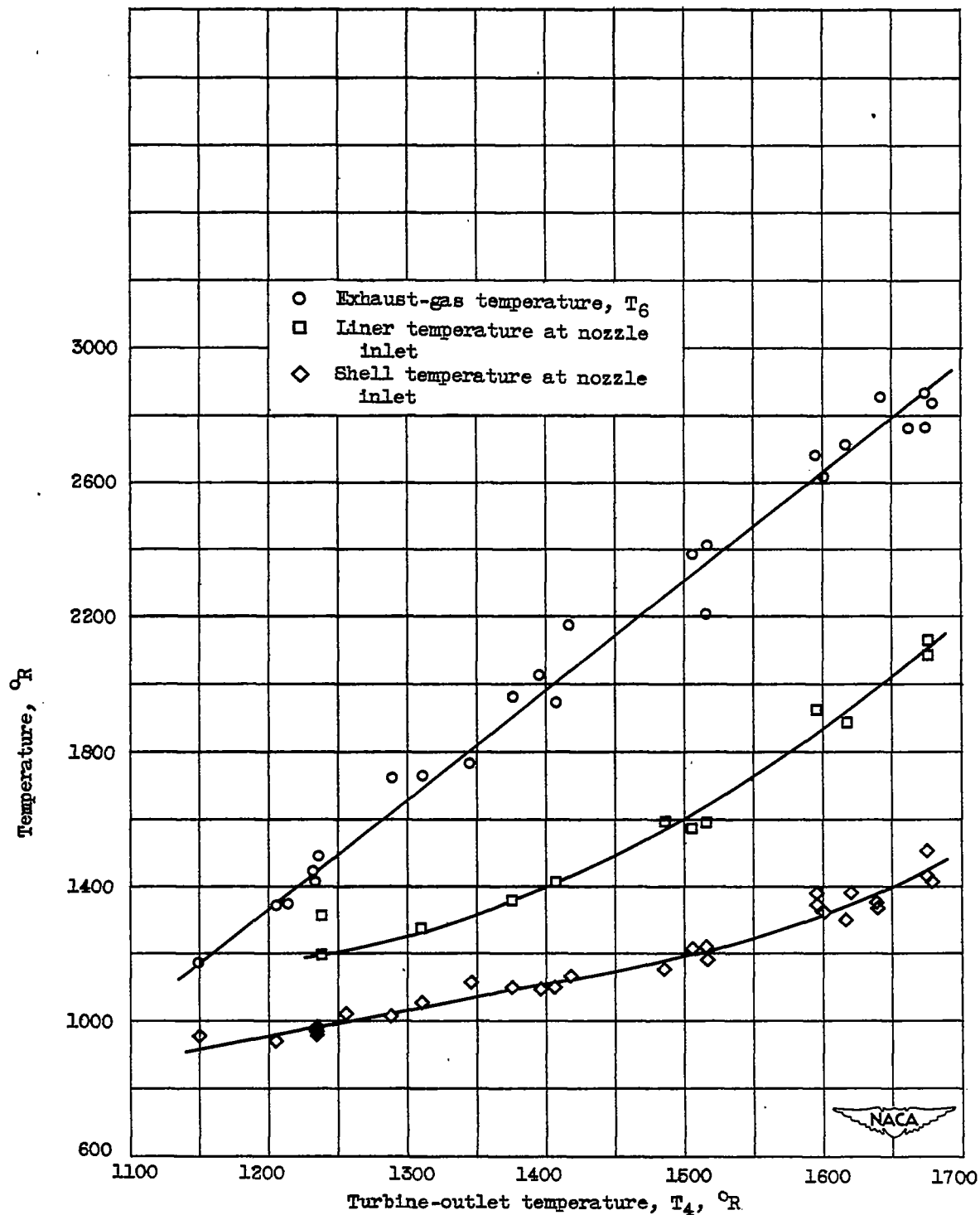
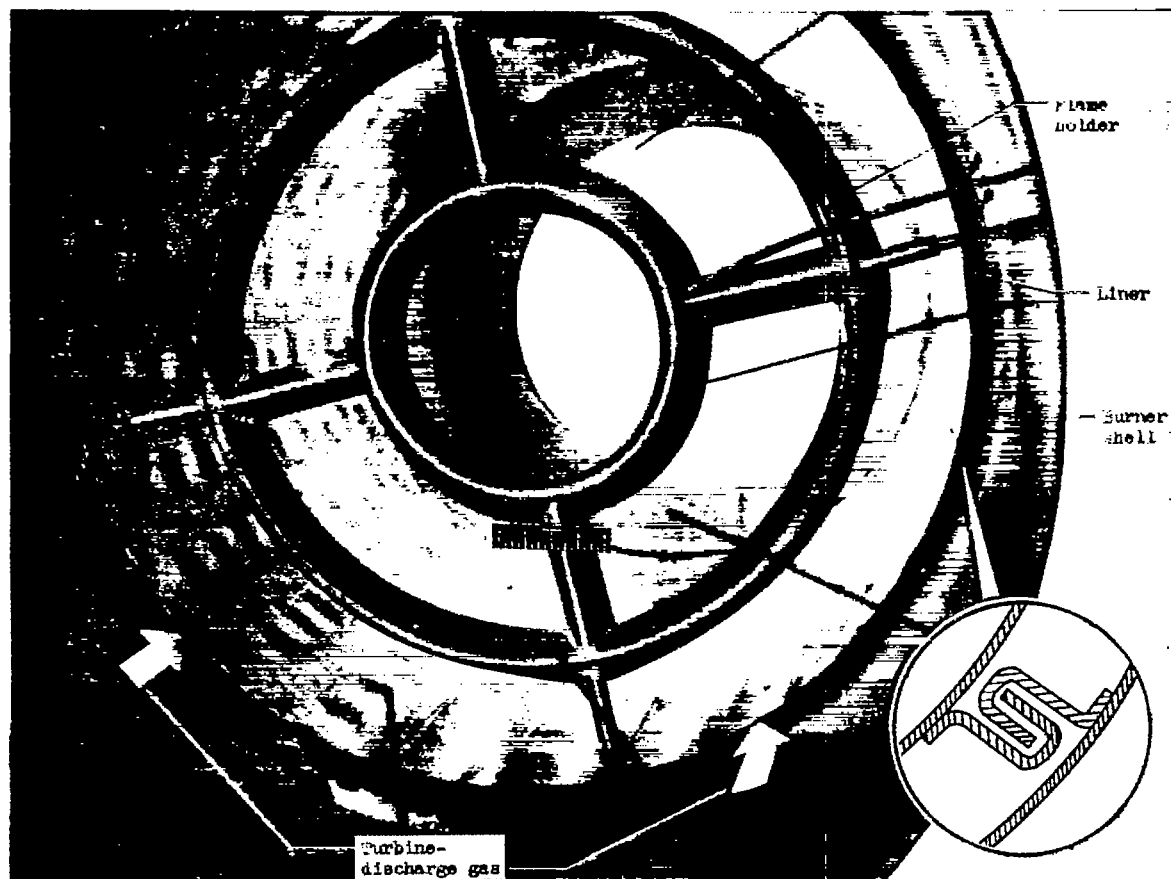
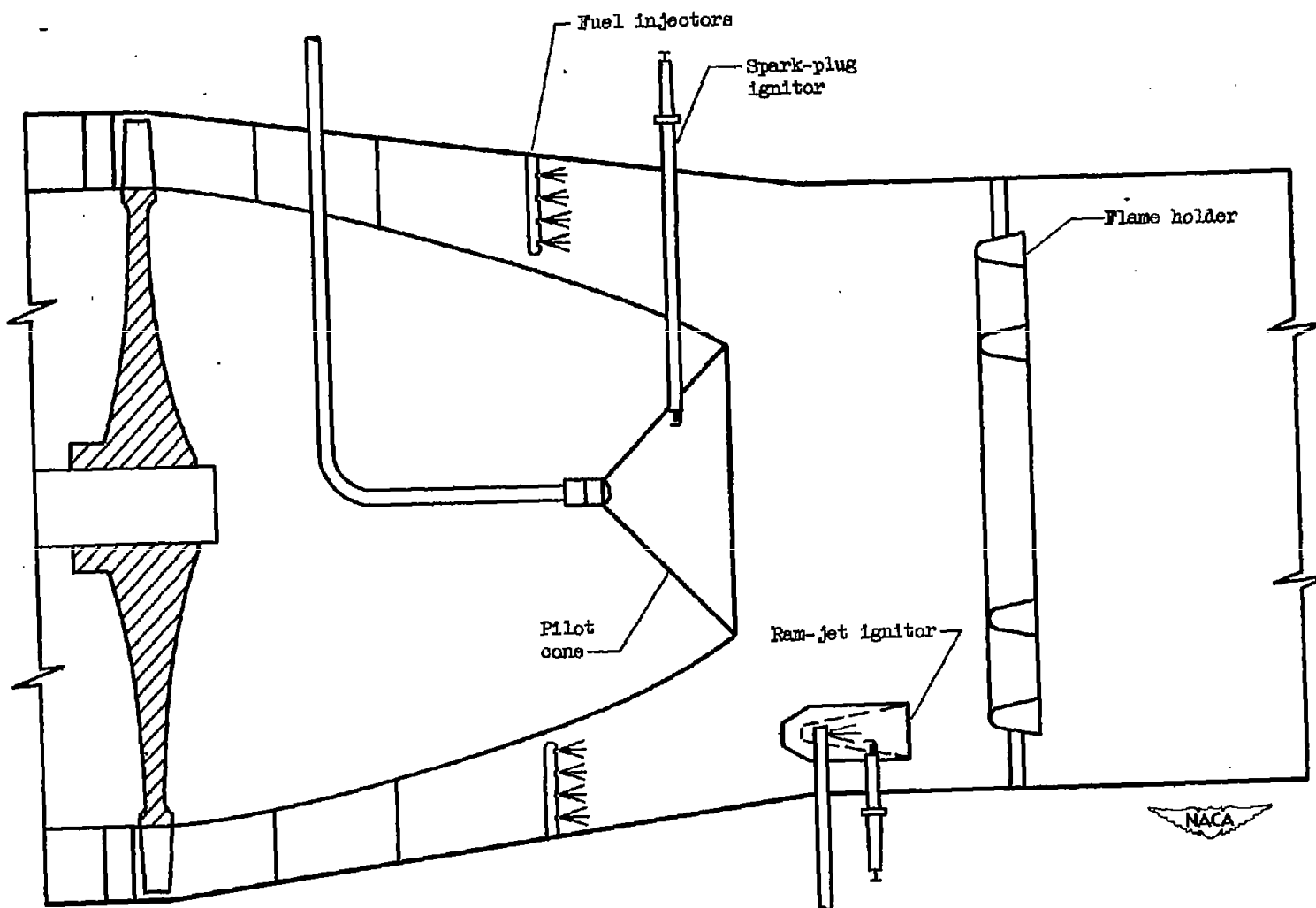


Figure 23. - Relation of exhaust-gas temperature and structure temperatures to turbine-outlet temperature for tail-pipe burner with cooling liner and fixed-area exhaust nozzle. Liner extended from burner inlet to within 2 inches of exhaust-nozzle outlet. Radial space 1/2-inch between liner and burner shell.



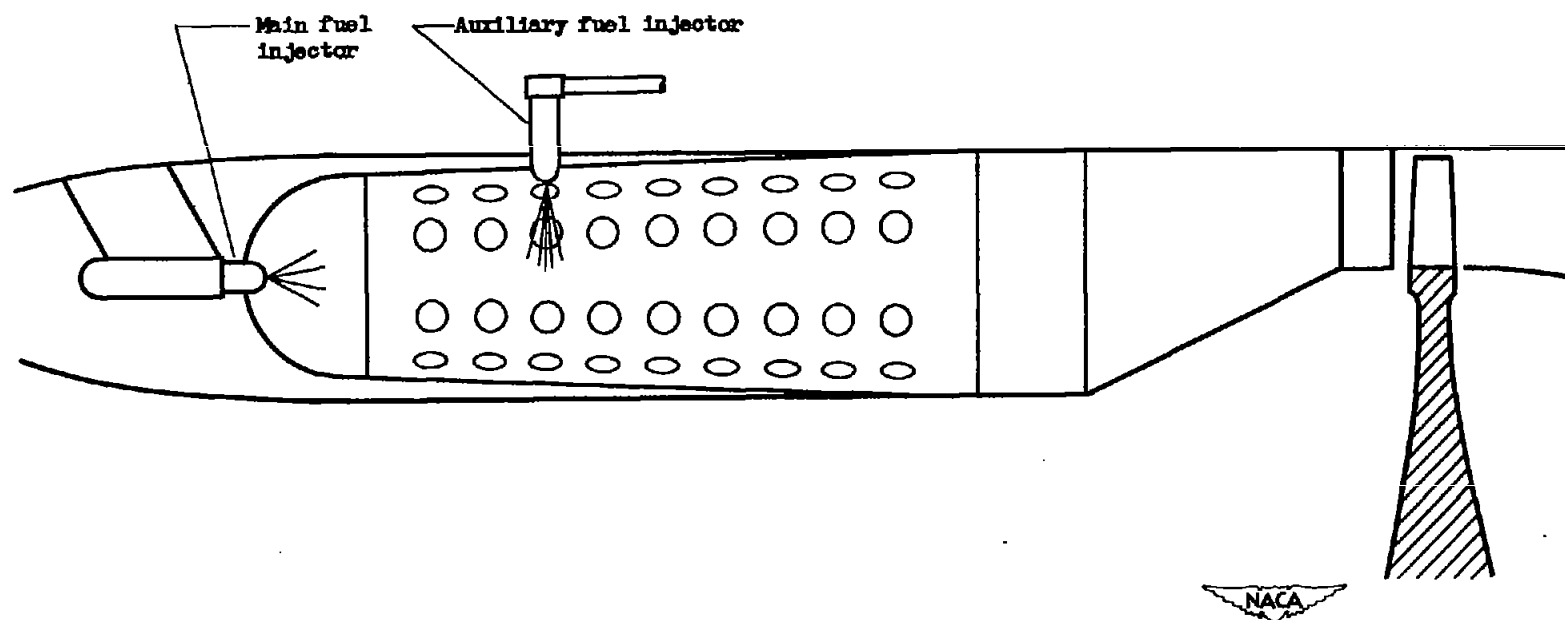
NACA
C-24818

Figure 24. - Installation of liner in tail-pipe burner.



(a) Tail-pipe systems.

Figure 25. - Schematic diagrams of tail-pipe burner ignition systems.



(b) "Hot-streak" system.

Figure 2S. - Concluded. Schematic diagrams of tail-pipe-burner ignition systems.

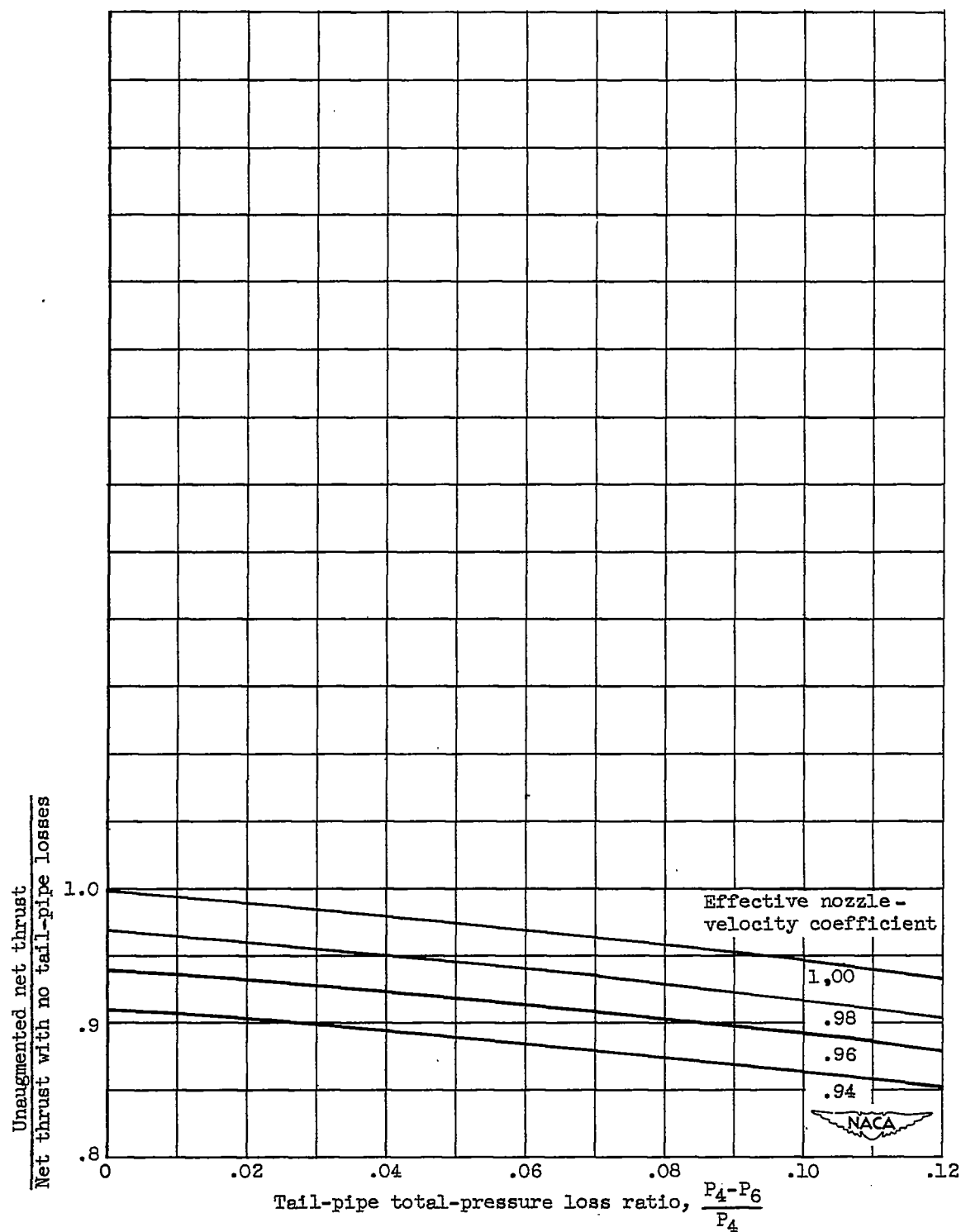


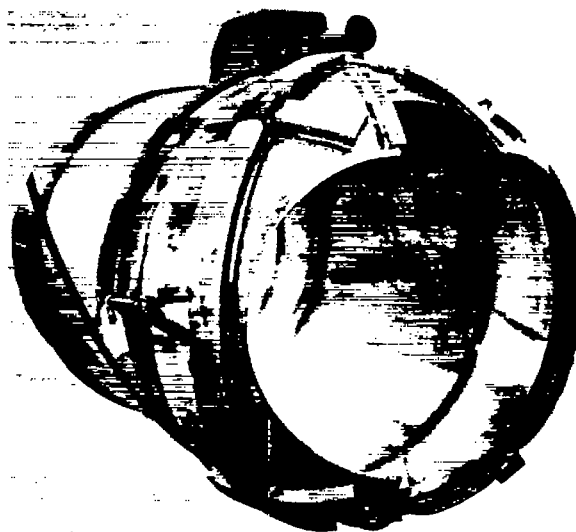
Figure 26. - Effect of tail-pipe total-pressure-loss ratio and exhaust-nozzle velocity coefficient on ratio of unaugmented net thrust to net thrust with no tail-pipe losses. Altitude, 35,000 feet; flight Mach number 0.8.

2058



NACA
C-21062

Nozzle A



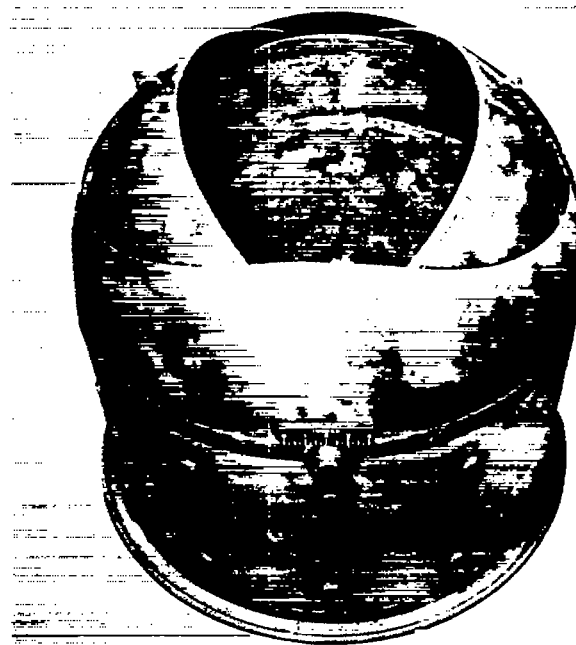
NACA
C-22479

Nozzle B



NACA
C-21060

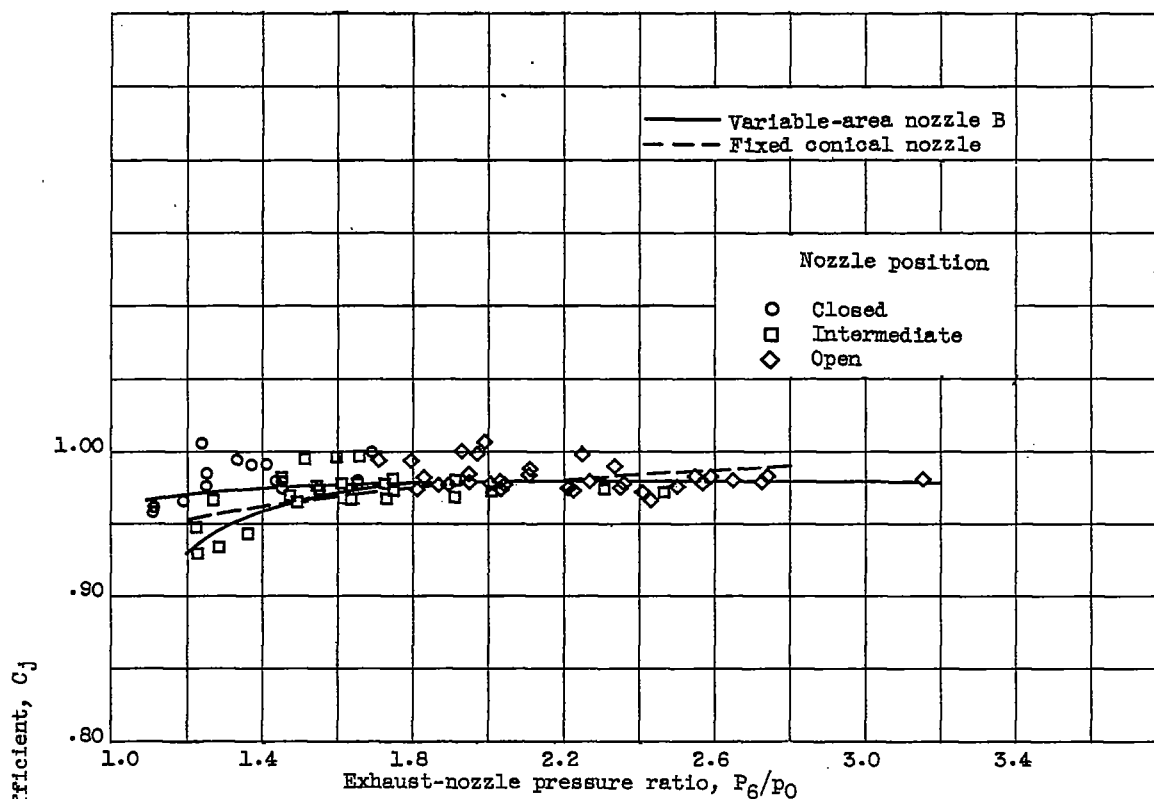
Nozzle C



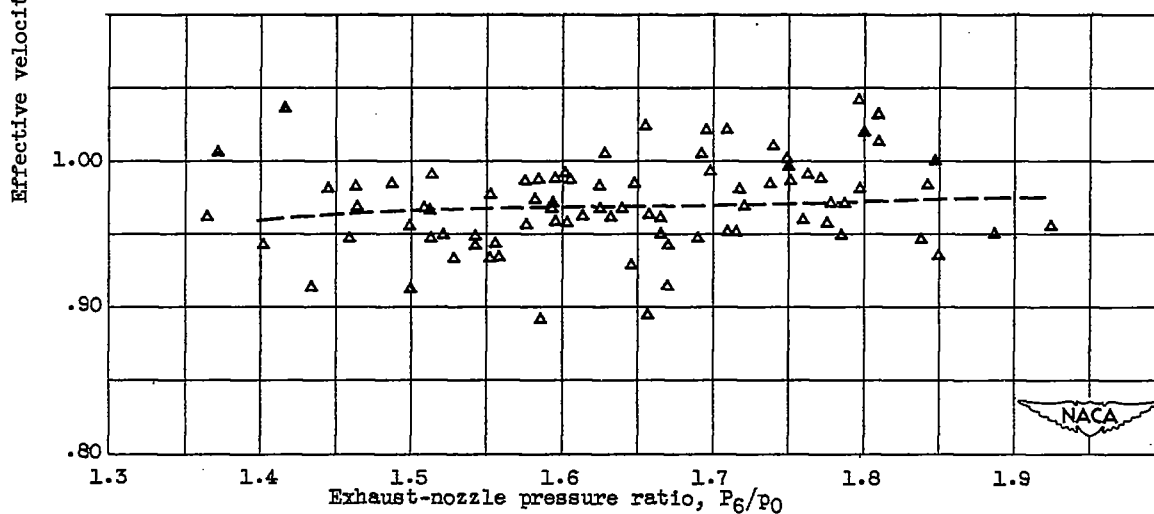
NACA
C-22245

Nozzle D

Figure 27. - Variable-area exhaust nozzles used with tail-pipe burning.



(a) Exhaust nozzle B.



(b) Exhaust nozzle D.

Figure 28.- Comparison of velocity coefficients of variable-area exhaust nozzles B and D with that of fixed conical nozzle.

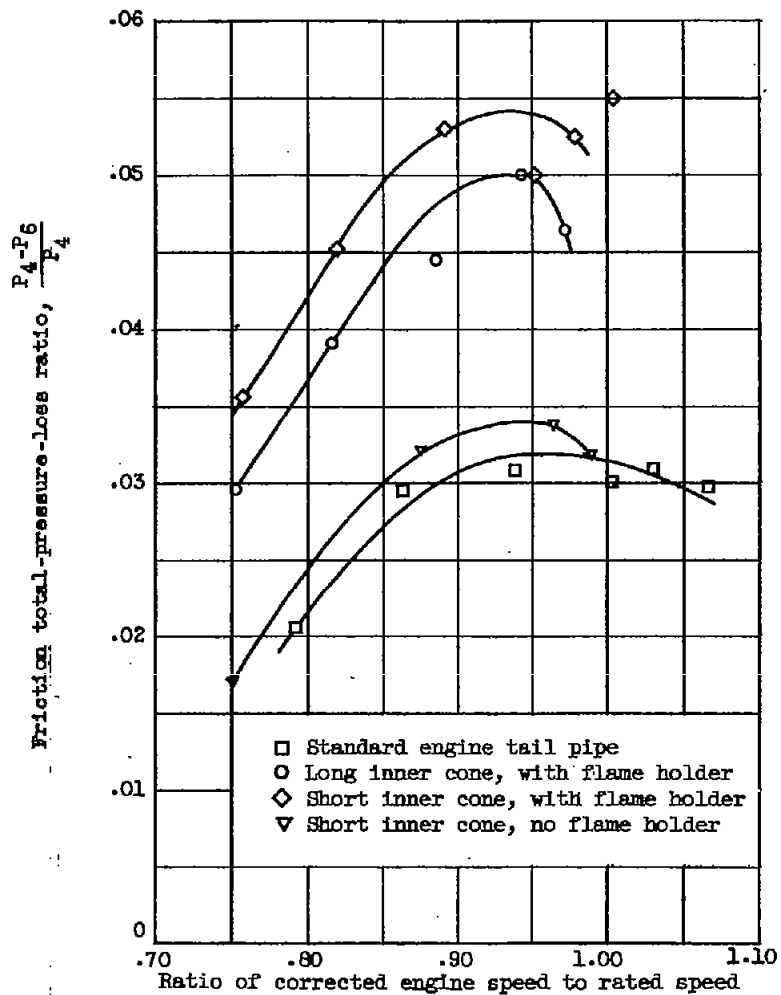
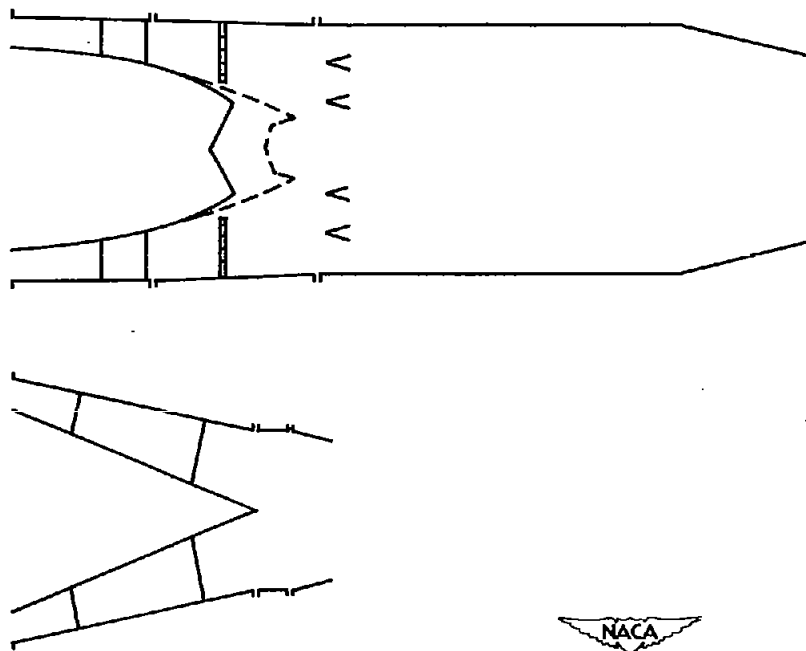
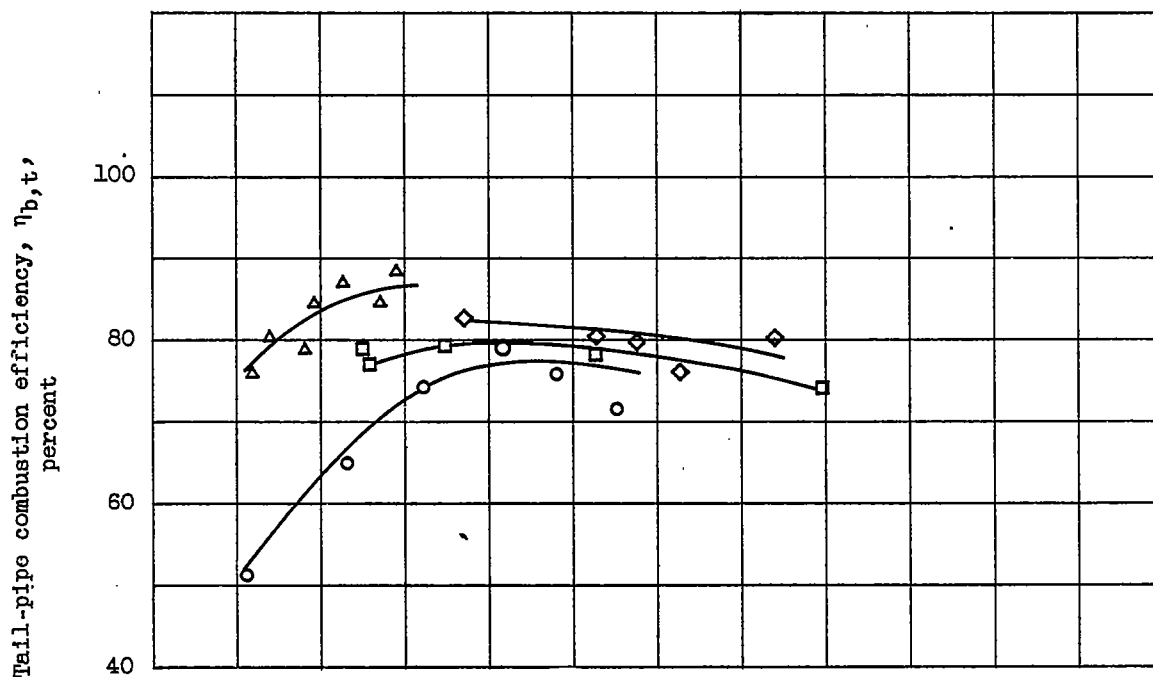


Figure 29. - Tail-pipe friction total-pressure-loss ratios with several diffusers.

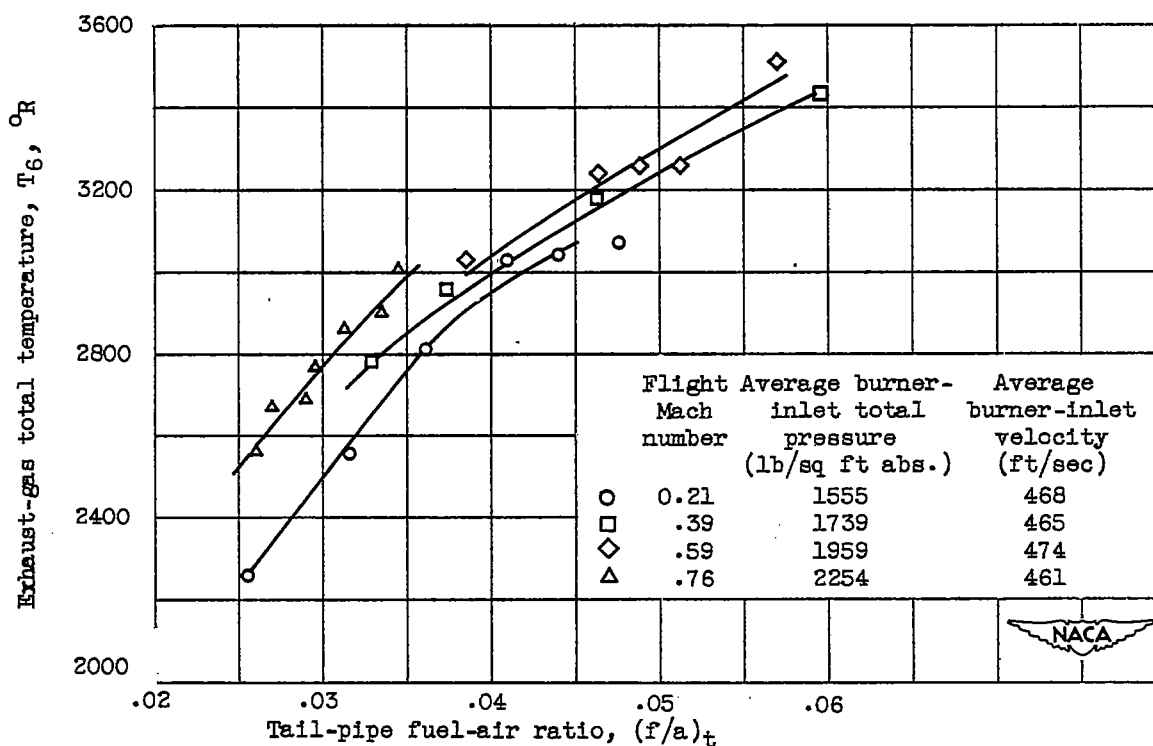


NACA

2058



(a) Tail-pipe combustion efficiency.



(b) Exhaust-gas total temperature.

Figure 30. - Over-all performance of typical tail-pipe burner. Altitude, 25,000 feet.

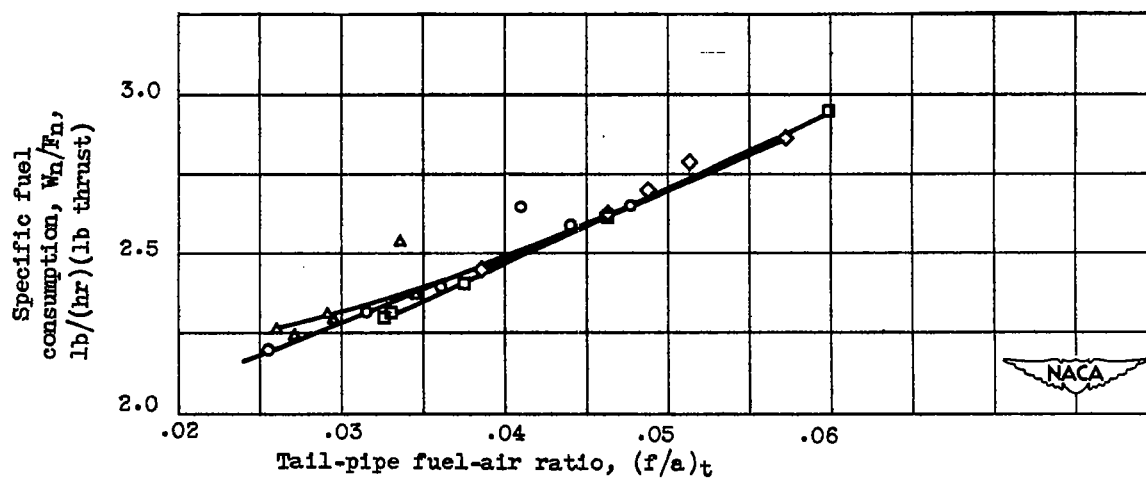
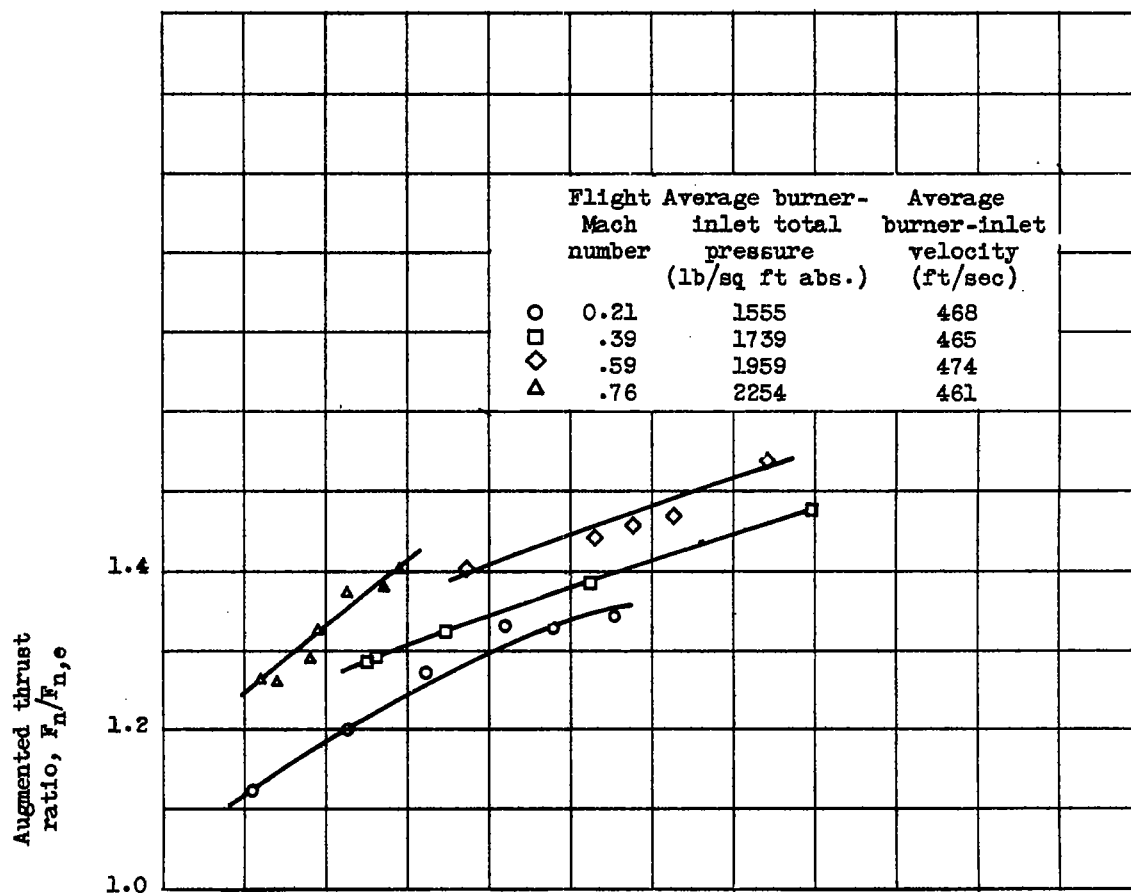
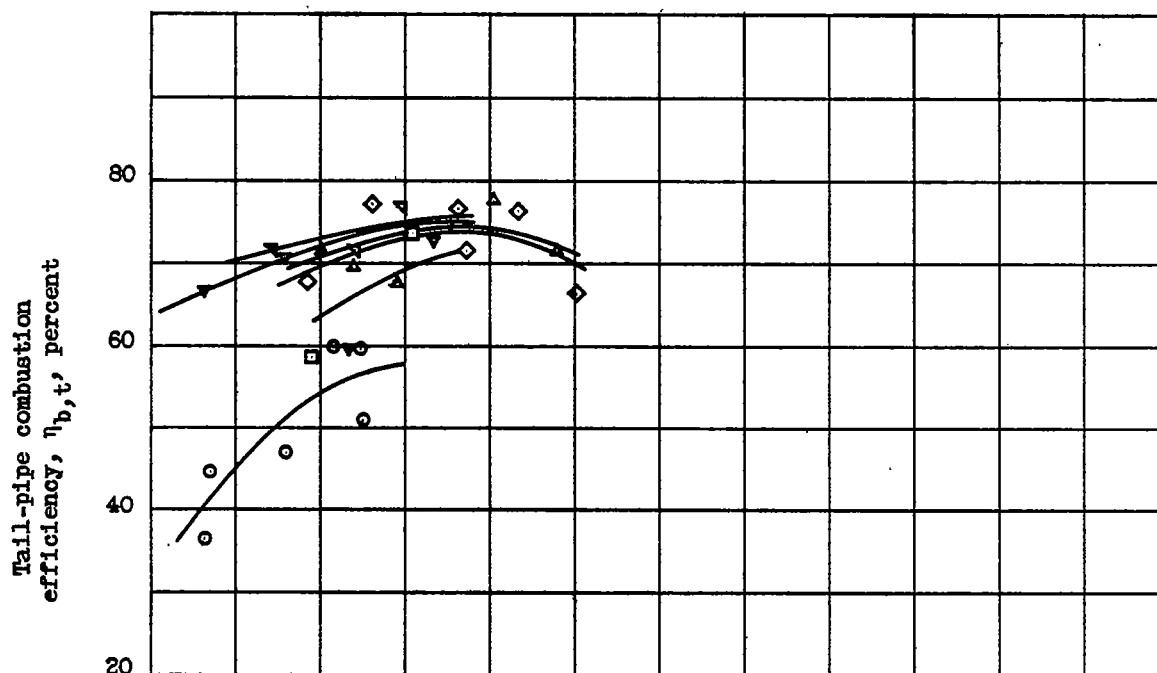
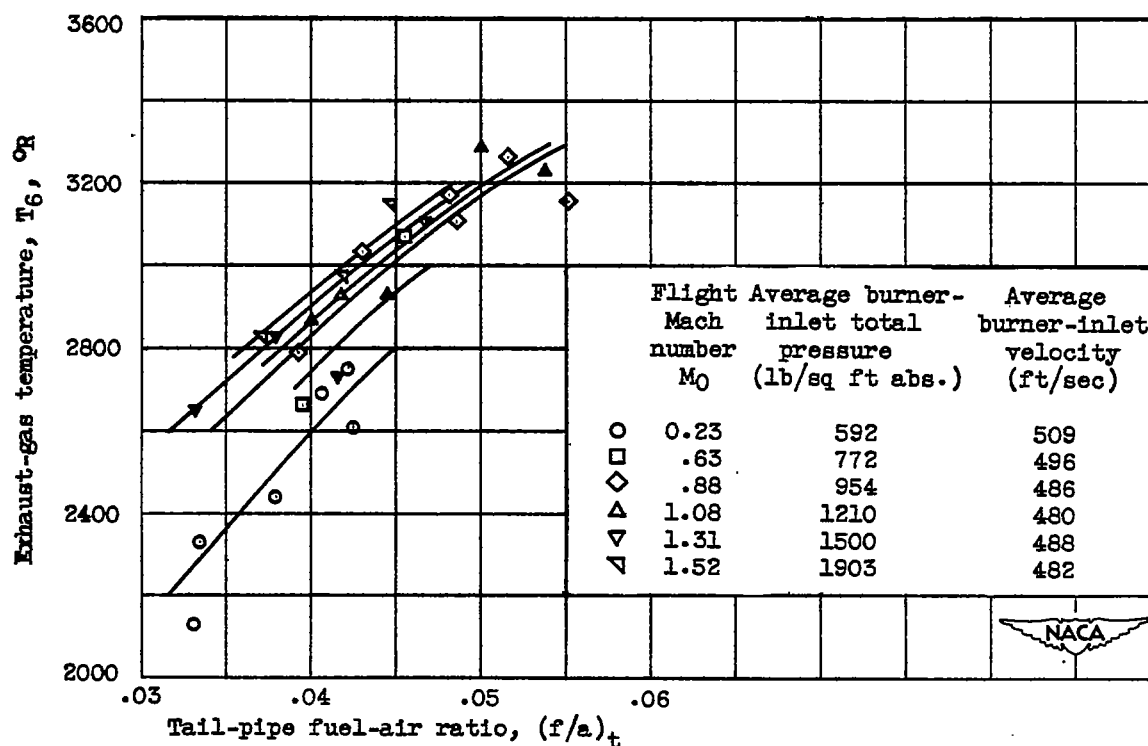


Figure 30. - Concluded. Over-all performance of typical tail-pipe burner.
Altitude, 25,000 feet.

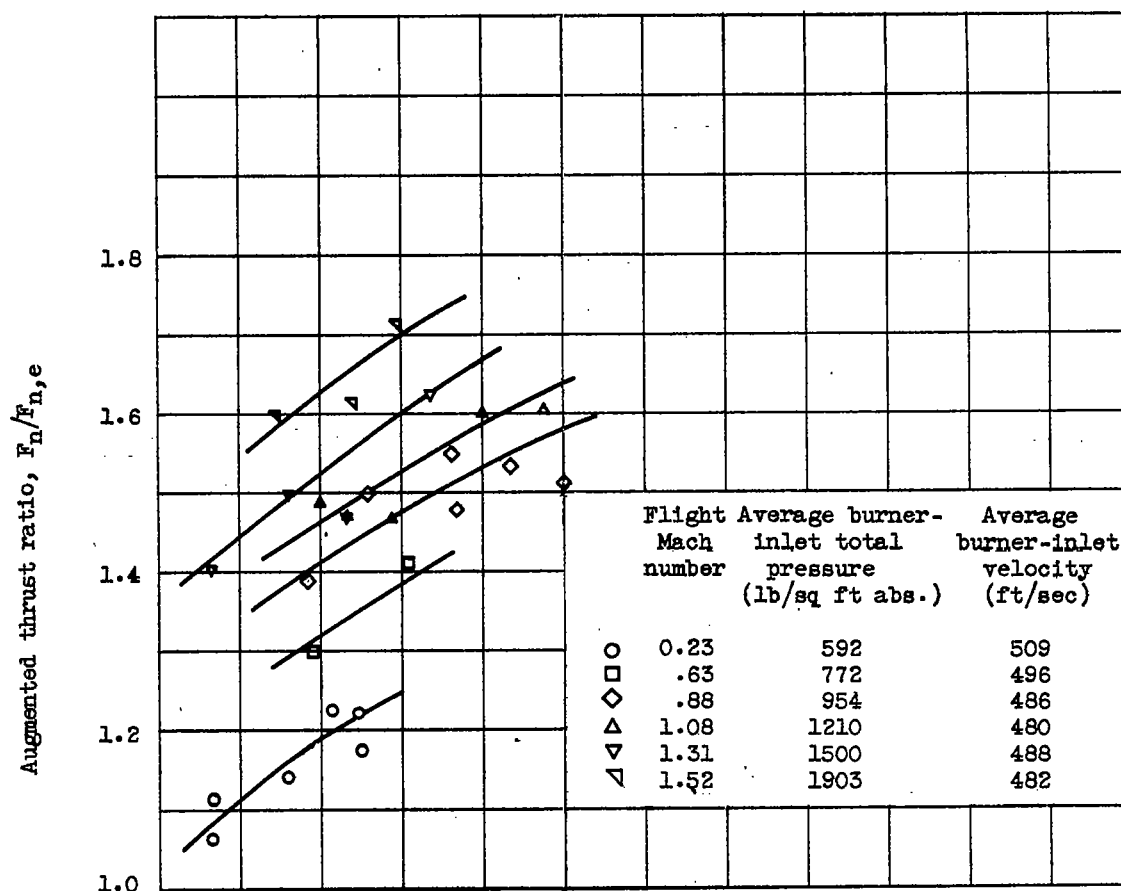


(a) Tail-pipe combustion efficiency.

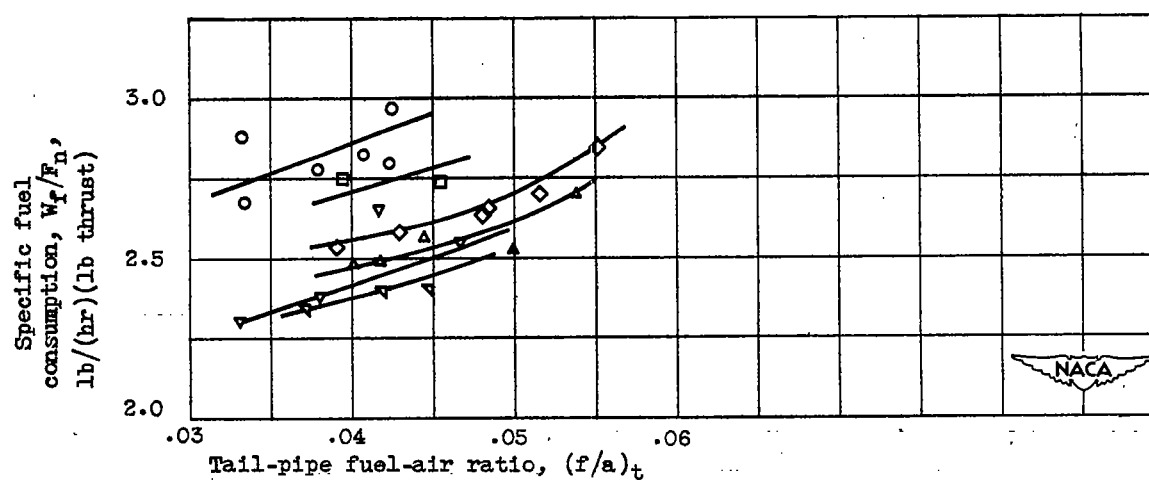


(b) Exhaust-gas total temperature.

Figure 31. - Over-all performance of typical tail-pipe burner. Altitude, 45,000 feet.



(c) Augmented thrust ratio.



(d) Specific fuel consumption.

Figure 31. - Concluded. Over-all performance of typical tail-pipe burner.
Altitude, 45,000 feet.

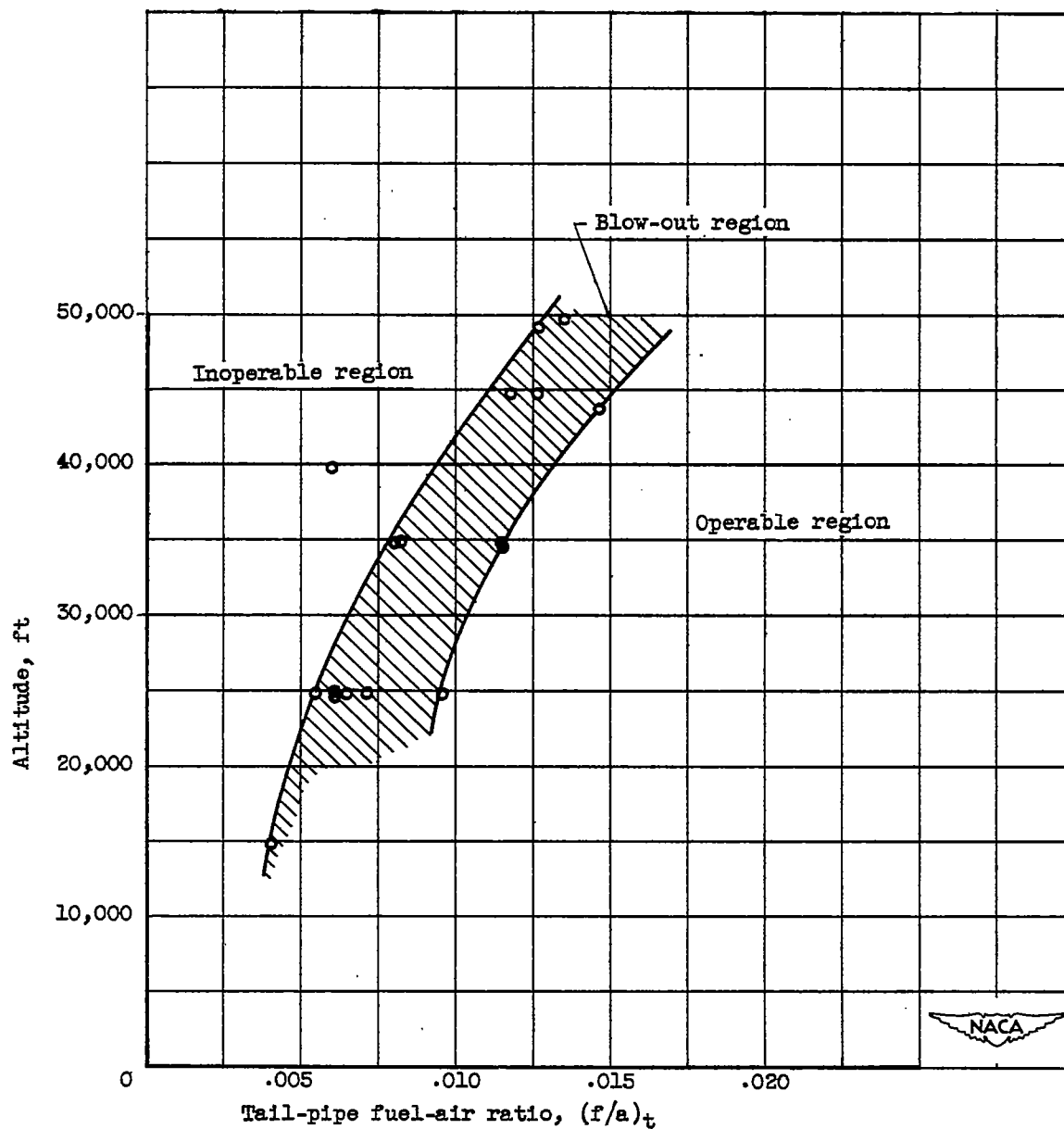


Figure 32. - Lean blow-out limits obtained with several configurations using AN-F-58 fuel at burner-inlet temperatures from 1250° to 1300° F. Flight Mach number, 0.19.